AVCO EVERETT RESEARCH LABORATORY

a division of
AVCO CORPORATION

A LIMIT ON STABLY TRAPPED PARTICLE FLUXES

C. F. Kennel and H. E. Petschek

RESEARCH REPORT 219
July 1965

supported jointly by
HEADQUARTERS
NATIONAL AERONAUTICS AND SPACE ADMINISTRATION
OFFICE OF SPACE SCIENCES
Washington, D. C.
under Contract No. NAS w-837

DEPARTMENT OF THE NAVY
OFFICE OF NAVAL RESEARCH
Washington 25, D. C.
under Contract No. Nonr-2524(00)

RESEARCH REPORT 219

A LIMIT ON STABLY TRAPPED PARTICLE FLUXES*

by

C. F. Kennel and H. E. Petschek

AVCO-EVERETT RESEARCH LABORATORY
a division of
AVCO CORPORATION
Everett, Massachusetts

July 1965

supported jointly by

HEADQUARTERS
NATIONAL AERONAUTICS AND SPACE ADMINISTRATION
OFFICE OF SPACE SCIENCES
Washington, D. C.

under Contract No. NAS w-837

DEPARTMENT OF THE NAVY
OFFICE OF NAVAL RESEARCH
Washington 25, D.C.

under Contract No. Nonr-2524(00)

* Submitted to Journal of Geophysical Research, July 27, 1965.

TABLE OF CONTENTS

ABSTRACT

10878

Whistler mode noise leads to electron pitch angle diffusion. Similarly, ion cyclotron noise couples to ions. This diffusion results in particle precipitation into the ionosphere and creates a pitch angle distribution of trapped particles which is unstable to further wave growth. Since excessive wave growth leads to rapid diffusion and particle loss, the requirement that the growth rate be limited to the rate at which wave energy is depleted by wave propagation allows an estimate of an upper limit to the trapped equatorial particle flux. Electron fluxes > 40 keV and proton fluxes > 120 keV observed on Explorers XIV and XII respectively obey this limit with occasional exceptions. Beyond $L = 4$, the fluxes are just below their limit, indicating that an unspecified acceleration source sufficient to keep the trapped particles near their precipitation limit exists. Limiting proton and electron fluxes are roughly equal, suggesting a partial explanation for the existence of larger densities of high energy protons than electrons. Observed electron pitch angle profiles correspond to a diffusion coefficient in agreement with observed lifetimes. The required equatorial whistler mode wide band noise intensity, $10^{-2}\ \gamma$, is not obviously inconsistent with observations, and is consistent with the lifetime and limiting trapped particle intensity.

1. INTRODUCTION

Recent observations of energetic electron precipitation from the magnetosphere to the atmosphere suggest that first adiabatic invariant violation must be responsible for the observed untrapping. Bursts of precipitation have been observed by balloon x-ray Bremsstrahlung measurement [Winckler, et al, 1963, Anderson and Milton, 1964] and direct > 40 keV electron flux measurements with Injun III [O'Brien, 1964] which exhibit 1/10 - 1 sec durations. This is roughly the time for these electrons to move from the equator to the ionosphere along a field line. Much shorter bursts than this would be unlikely, even if these electrons were thrown instantaneously into the loss cone. This suggests that first invariant violation, which can occur on a 10^{-4} sec time scale, is a likely explanation, since violation of the second invariant would probably require several bounce periods and therefore could not produce such short bursts.

McDiarmid and Budzinski [1964] argue that the similarity of electron energy spectra at 1000 km heights and in the equatorial plane together with the short observed lifetimes [10^{3-5} sec, O'Brien, 1962] suggest that changes in pitch angle without a change in energy, (first invariant violation) are necessary. Conservation of this invariant during the time the particle lowers its mirror points (10^{3-5} sec) would imply a total energy increase in this time of a factor of 10^{3}. The observed spectral similarities would then be difficult to explain.

The conditions for first adiabatic invariant violation are quite restrictive. A given particle must see fluctuations near its own gyro frequency. This immediately suggests high frequency fluctuations in the whistler and ion cyclotron modes, for electrons and ions respectively, since they have the appropriate frequency range. In this way, Dungey [1963], and Cornwall [1964] have suggested that external sources of whistler radiation, such as atmospherics, may account for energetic electron lifetimes in the vicinity of $L = 2$. Similarly, Dragt [1961], Wentzel [1961], Chang and Pearlstein [1964] and others have suggested that hydromagnetic waves will scatter protons out of the Van Allen Belts.

The difficulty at present does not lie in identifying a pitch angle scattering mechanism, but in evaluating quantitatively its effects, and in finding restrictive and conclusive comparisons with observation. Estimation of the fluctuation amplitude requires knowledge of external wave sources, such as atmospherics, or of the nonlinear process which limits the amplitude, if wave energy is to be internally generated by an instability. In this regard, Cornwall [1965] and Brice [1965] have observed that the whistler mode will be unstable if the pitch angle distribution is sufficiently anisotropic. Thus wave energy can be generated within the magnetosphere, provided an anisotropic pitch angle distribution can be maintained. In this paper we attempt a quantitative investigation of those effects related to the presence of waves which are essentially independent of the specific wave source.

The limitation of wave growth as well as the pitch angle diffusion due to waves requires a nonlinear treatment. A basic simplification of plasma turbulence is that it is often low level and can be treated accurately to second order in wave amplitude. Therefore, many fundamental properties are defined in terms of the familiar linear (first order) theory for wave propagation and growth. In Section 2, we review the linear theory of the whistler, ion cyclotron and magnetosonic modes, concentrating on resonant effects which lead to wave growth. The stability properties depend primarily upon particles in cyclotron resonance, whose velocity parallel to the magnetic field Doppler shifts the wave frequency to their cyclotron frequency. Pitch angles of these particles are thereby altered. Wave growth will occur when the pitch angle distribution of resonant particles is sufficiently anisotropic. The magnitude of the growth rate is determined both by the pitch angle anisotropy and by the fraction of particles which are resonant.

Simple physical arguments indicate that resonant wave growth is nonlinearly limited. For instance, resonant particle energy and wave energy are conserved together. If one gains energy, the other loses. Only the pitch angle anisotropy energy of resonant particles is available for whistler and ion cyclotron wave growth. Since this is a small fraction of the total kinetic energy, these waves may grow only to a low level before they exhaust the energy available to them. The fact that waves take energy from particles appears in linear theory as the resonant instability; the effect of the waves

back on the particle distribution is necessarily nonlinear. In Section 3, we show that the particle distribution for an infinite plasma evolves by diffusion primarily in pitch angle towards the marginal stability configuration-pitch angle isotropy - at a rate proportional to the square of the resonant wave amplitude. Since there is little diffusion in energy, these waves cannot be an acceleration mechanism.

Pitch angle diffusion in spatially finite plasmas differs significantly from the infinite plasma case. In Section 4 we discuss the steady state pitch angle distribution appropriate to the finite magnetosphere. Since particles which reach the loss cone are lost to the atmosphere, the steady pitch angle distribution will necessarily be anisotropic. Since predominantly parallel energy is lost to the atmosphere, this anisotropy has the appropriate sign to be unstable and thus can generate its own wave amplitude. In order that pitch angle diffusion be self-sustaining, both the particles and waves which escape must be replaced. There must be acceleration mechanisms for the particles, and the wave growth rate must adjust, not to zero as for the infinite plasma, but to a small positive value in order to replace lost wave energy.

Although the rate at which particles diffuse towards the loss cone depends upon the magnitude of the diffusion coefficient, and therefore on wave energy, the shape of the steady state pitch angle distribution outside the loss cone is essentially independent of the diffusion coefficient, so long as it is nonzero. (In steady heat conduction the heat flux depends upon the magnitude of the thermal conductivity; however, the temperature distribution is independent of conductivity when the temperature is specified at the boundaries. Similarly, the pitch angle anisotropy is fixed in steady turbulent diffusion). The wave growth rate can then depend only upon the number of resonant particles. This number must adjust be balancing acceleration with precipitation so that the growth rate just replaces escaping wave energy. If the growth rate is too large, wave energy will accumulate, rapidly enhancing particle precipitation, thereby reducing the growth rate to that necessary to maintain a steady wave distribution. Therefore, there is an upper limit to stably trapped particle fluxes. We estimate this upper limit in Section 5 by equating the wave growth rate to the wave escape rate. Instabilities are important when trapped fluxes are near this limit. Since observed fluxes of > 40 keV

electrons satisfy the calculated upper limit, whistler mode pitch angle diffusion probably limits the electron intensities. Since their intensities are always near but below their upper limit beyond $L = 5$, acceleration must occur all the time there, and so therefore does precipitation. Higher energy electrons are less often near instability because their fluxes are usually well below the flux needed for self-excitation.

The corresponding limit for protons is discussed in Section 6. It is again found that experiments confirm this upper limit. Observed fluxes of > 120 keV protons are close to but do not exceed the limit, thus implying that a sufficient acceleration source also exists for protons. It is also significant that the calculated limiting fluxes are comparable for electrons and ions. The observation of larger proton than electron densities can then be explained by the fact that both species are apparently accelerated to their limiting density; however, the limiting proton density is significantly larger than the limiting electron number density.

We emphasize that this estimate of the maximum stably trapped flux involves only a comparison of the wave growth rate with the wave escape rate, which in turn depends primarily on the wave group velocity and the length of a line of force. It is clear the the maximum trapped flux cannot depend upon the acceleration mechanisms which create it. If acceleration is continual, the trapped particle distribution will eventually reach and be limited to a maximum intensity and the observed trapped particle intensity should then be insensitive to further changes in the acceleration mechanism. On the other hand, the precipitation rate will be strongly correlated with acceleration, when the trapped fluxes are near self-limitation. In this paper we will not discuss the particle acceleration mechanisms since they are not clearly understood at present.

Besides trapped equatorial omnidirectional intensities, the other information available for study is pitch angle distributions obtained in and near the loss cone by polar orbit satellites. In Section 7 we show that the observed > 40 keV electron pitch angle profiles are consistent with independent estimates of the lifetimes. Although the pitch angle distribution outside the loss cone is virtually independent of the magnitude of the diffusion coefficient, the distribution inside depends upon the ratio of the diffusion time

to the time of loss to the atmosphere. Therefore, the measured loss cone profiles [O'Brien, 1964] estimate a diffusion coefficient and a particle lifetime. The wave intensity required to produce these lifetimes is at least an order of magnitude larger than that observed near the Earth, if waves propagate completely trapped on a tube of force without attenuation. However, pitch angle scattering occurs predominantly near the equator, and much of the wave energy so generated may be lost before it reaches the ionosphere. In Section 8, we show that these theoretically derived wave intensities combined with the observed rate of particle energy loss from the magnetosphere permit an estimate of the growth rate which is consistent with the known wave escape rate. Thus the observed pitch angle distributions, lifetimes, trapped particle fluxes, and the inferred wave intensity appear to be mutually consistent.

2. LINEAR PROPAGATION AND STABILITY OF THE WHISTLER AND ION CYCLOTRON MODES

2.1 Introduction

In Section 3, we shall show that the nonlinear behavior of weak turburlence in the whistler and ion cyclotron modes involves the linear theory growth rate. In this section, we review the linear theory. Several similar analyses have been performed [Sagdeev and Shafranov, 1961, Stix, 1962, Chang, 1963]. It is repeated here principally to define notation and review the physical picture of the instability. We shall indicate that the whistler mode is unstable when the electron pitch angle distribution is sufficiently anisotropic, with more energy perpendicular than parallel to the magnetic field, and that the ion cyclotron mode grows when there is similar ion pitch angle anisotropy. In each case, the growth rates are non-negligible only when an appreciable fraction of the particle distribution is near cyclotron resonance.

Since we are interested in the high frequency properties of a collision-free plasma, the Vlasov-Maxwell equations for a plasma of ions and electrons (denoted by $^+$, $^-$ respectively) must be the starting point for this analysis.

$$\frac{\partial f^{\pm}}{\partial t} + \underset{\sim}{v} \cdot \underset{\sim}{\nabla} f^{\pm} \pm \frac{e}{M^{\pm}} \left[\underset{\sim}{E} + \frac{\underset{\sim}{v} \times \underset{\sim}{B}}{c} \right] \cdot \frac{\partial f^{\pm}}{\partial \underset{\sim}{v}} = 0 \qquad (2.1)$$

$$\nabla \cdot \underset{\sim}{E} = 4\pi e \int d^3v \, (f^+ - f^-) \tag{2.2}$$

$$\nabla \times \underset{\sim}{E} = -\frac{1}{c} \frac{\partial \underset{\sim}{B}}{\partial t} \tag{2.3}$$

$$\nabla \times \underset{\sim}{B} = \frac{4\pi e}{c} \int d^3v \, \underset{\sim}{v} (f^+ - f^-) + \frac{1}{c} \frac{\partial \underset{\sim}{E}}{\partial t} \tag{2.4}$$

$$\nabla \cdot \underset{\sim}{B} = 0 \tag{2.5}$$

where $f^{\pm}(\bar{x}, \bar{v}, t)$ are the one particle distribution function of each species, e is the electronic charge, $M^{\pm}$ is the mass of each species. Gaussian units are used throughout.

Since the wavelengths relevant to pitch angle scattering are necessarily much shorter than typical macroscopic scale lengths in the magnetosphere, it is a good approximation to treat waves propagating locally in an infinite uniform plasma immersed in a strong magnetic field pointing in, say, the z direction. As will be indicated below, the waves of primary interest for pitch angle scattering propagate parallel to the magnetic field. Since this is also the simplest case algebraically, we discuss it first and later comment briefly on the nonparallel case.

Assuming there are no electric field, spatial gradients, time variations, and only a z-component of the magnetic field in the equilibrium, the equilibrium distribution function $F^{\pm}$ must obey

$$B_o (\underset{\sim}{v} \times \underset{\sim}{e}_z) \cdot \frac{\partial F^{\pm}}{\partial \underset{\sim}{v}} = 0 \tag{2.6}$$

where $\bar{e}_z$ is a unit vector in the magnetic field direction. Transforming to a cylindrical velocity space coordinate system centered about the equilibrium

magnetic field, $v_x = v_\perp \cos\phi$, $v_y = v_\perp \sin\phi$, $v_z = v_\parallel$, ($v_\perp$ is the component v perpendicular to the magnetic field, $v_\parallel$ the parallel component) (2.6) reduces simply to $\partial F^{\pm}/\partial \phi = 0$. The equilibrium distribution function is therefore independent of the Larmor phase angle. If we now allow small perturbations of the form:

$$f^{\pm}_{\sim}(\underset{\sim}{x}, \underset{\sim}{v}, t) = N F^{\pm}_{\sim}(\underset{\sim}{v}) + \delta f^{\pm}_{\sim}(\underset{\sim}{v})\, e^{i(kz - \omega t)} \tag{2.7}$$

$$\underset{\sim}{B}(\underset{\sim}{x}, t) = B_o \underset{\sim}{e}_z + \underset{\sim}{\delta B}\, e^{i(kz - \omega t)} \tag{2.8}$$

$$\underset{\sim}{E}(\underset{\sim}{x}, t) = 0 + \underset{\sim}{\delta E}\, e^{i(kz - \omega t)} \tag{2.9}$$

and

substitute these into (2.1) through (2.5), dropping nonlinear terms in the perturbation, (2.1) through (2.5) can be reduced to the following single matrix equation for the electric field components (in index notation)

$$[n^2 \delta_{\alpha\beta} - n_\alpha n_\beta - \epsilon_{\alpha\beta}]\ \delta E_\beta = 0\ ;\ \alpha, \beta = 1, 2, 3 \tag{2.10}$$

where $n_\alpha = ck_\alpha/\omega$, the index of refraction, and $\epsilon_{\alpha\beta}(\omega, k)$ is the dielectric tensor

$$\epsilon_{\alpha\beta}(\omega, k) = \delta_{\alpha\beta} - \sum_{+,-} \frac{(\omega_p^{\pm})^2}{\omega} \int_0^\infty v_\perp\, dv_\perp \int_0^\infty dv_\parallel \int_0^{2\pi} d\phi$$

$$v_\alpha L^{-1} \left\{ \frac{\partial F^{\pm}}{\partial v_\beta} \left(1 - \frac{kv_\parallel}{\omega}\right) + v_\beta k \frac{\partial F^{\pm}}{\partial v_\parallel} \right\} \tag{2.11}$$

where $\sum_{+,-}$ denotes a sum over species, $\omega_p^{\pm} = \sqrt{4\pi N e^2/M^{\pm}}$ = the plasma frequency of each species. Notice that the equilibrium velocity distribution $F^{\pm}$ is normalized to one. L^{-1} is the inverse of the linearized Vlasov operator

$$L^{-1} = \frac{1}{\Omega^{\pm}} e^{\frac{-i(kv_{\parallel} - \omega)\phi}{\Omega^{\pm}}} \int^{\phi} d\phi' \, e^{\frac{+i(kv_{\parallel} - \omega)\phi'}{\Omega^{\pm}}} \tag{2.12}$$

where $\Omega^{\pm} = \pm e B/M^{\pm} c$, the cyclotron frequency for each species.

The dispersion relation is simply Det $(n^2 \delta_{\alpha\beta} = n_\alpha n_\alpha - \epsilon_{\alpha\beta}) = 0$. For parallel propagation, this determinant factors into two parts. One involves longitudinal oscillations involving only z components of the electric field. This leads to plasma oscillations and the ion acoustic mode and is of no further interest here. The other part is for transverse electromagnetic oscillations, involving E_x and E_y. If we now assume that these modes are circularly polarized about the magnetic field so that $E_x \pm i E_y$ are convenient independent variables, the dispersion relation once again factors into two modes, one for each polarization:

$$n^2 = R \, , \; n^2 = L$$

$$\begin{pmatrix} R \\ L \end{pmatrix} = 1 - \pi \sum_{+,-} \frac{(\omega_p^{\pm})^2}{\omega} \int_0^{\infty} v_{\perp}^2 \, dv_{\perp} \int_{-\infty}^{+\infty} dv_{\parallel}$$

$$\left[\frac{\partial F^{\pm}}{\partial v_{\perp}} - \frac{k}{\omega} \left(v_{\parallel} \frac{\partial F^{\pm}}{\partial v_{\perp}} - v_{\perp} \frac{\partial F^{\pm}}{\partial v_{\parallel}} \right) \right] \cdot \begin{pmatrix} \dfrac{1}{kv_{\parallel} - \omega - \Omega^{\pm}} \\ \\ \dfrac{1}{kv_{\parallel} - \omega + \Omega^{\pm}} \end{pmatrix} \tag{2.13}$$

Since the equilibrium distributions $F^{\pm}_{-}$ are independent of the Larmor phase angle ϕ, it was convenient to eliminate the operation L^{-1} by performing the ϕ integration before writing (2.13). At low frequencies, $\omega/\Omega^{+} << 1$, $n^2 = R$ is the magnetosonic mode; when $\Omega^{+} << \omega < |\Omega^{-}|$, $n^2 = R$ is the whistler mode. When $\omega/\Omega^{+} << 1$, $n^2 = L$ is the anisotropic Alfven wave; when the wave frequency approaches the ion gyro frequency, this is called the ion cyclotron wave. We discuss first the whistler mode and then by analogy the ion cyclotron mode.

2.2 Whistler Mode

When the plasma pressure is much smaller than the magnetic pressure, a good approximation to the real part of the index of refraction assumes the plasma to be cold. In other words, we substitute in (2.13)

$$F^{\pm}_{-} = \frac{1}{2\pi}\,\delta(v_{\perp})\,\delta(v_{\parallel}) \tag{2.14}$$

where the cylindrical velocity space normalization requires

$$\int_{0}^{2\pi} d\phi \int_{0}^{\infty} v_{\perp}\, dv_{\perp}\, \delta(v_{\perp}) \int_{-\infty}^{+\infty} \delta(v_{\parallel}) dv_{\parallel} = 1 \tag{2.15}$$

After substitution, the first term in the numerator of (2.13), involving $v_{\perp}^{2}\,\partial F^{\pm}_{-}/\partial v_{\perp}$, can be integrated by parts once to give $-1/\pi$. The other two terms vanish for the zero-temperature case. Thus $n^2 = R$ reduces to

$$\frac{c^2 k^2}{\omega^2} = n^2 = 1 - \frac{(\omega_p{}^{+})^2}{\omega(\omega+\Omega^{+})} - \frac{(\omega_p{}^{-})^2}{\omega(\omega+\Omega^{-})} \tag{2.16}$$

The sign of the particles species is incorporated into $\Omega^{\pm}_{-}(=\pm eB/M^{\pm}_{-}c)$. When the wave frequency is well above the ion gyro frequency, but below the electron gyro frequency, so that $\Omega^{+} << \omega < |\Omega^{-}|$, the ion contribution

to (2.16) is a factor m^-/M^+ smaller than the electron contribution and may be neglected. Furthermore, if the electron plasma frequency is large, so that $\left|\omega_p^-/\Omega^-\right| >> .1$, the phase velocity is much smaller than the velocity of light, and $n^2 = R$ is approximately

$$\mathrm{Re}\,(n^2) \approx \frac{(\omega_p^-)^2}{\omega(\left|\Omega^-\right| - \omega)} \tag{2.17}$$

Similarly, we can show that the mode $n^2 = L$ is evanescent above the ion gyro frequency.

Neglecting all thermal velocities has led to a simple expression for the real part of the index of refraction, which depends only upon the strength of the external magnetic field and the total particle density. However, the growth or damping of these waves is necessarily a finite velocity dispersion effect since it depends only upon those electrons in cyclotron resonance. The cyclotron resonance phenomenon arises from the resonant denominators in (2.13), $1/(kv_{\parallel} - \omega - \Omega^{\pm})$. Where these denominators are zero, the velocity space integration picks up an imaginary part. For electron gyroresonance, the resonant velocity V_R is defined by

$$k V_R = \omega - \left|\Omega^-\right| \tag{2.18}$$

The velocity of these particles parallel to the external magnetic field Doppler shifts the wave frequency to their gyro frequency. These electrons may therefore have their magnetic moment efficiently altered. For some purposes it is helpful to rewrite (2.18) in terms of the energy associated with the parallel motion of the resonant particle. Using the dispersion relation (2.14), the resonance condition for electrons, (2.18), may be written

$$E_R = \frac{1}{2} m^- V_R^2 = E_c \frac{\left|\Omega^-\right|}{\omega} \left(1 - \frac{\omega}{\left|\Omega^-\right|}\right)^3 \tag{2.19}$$

$E_c = B^2/8\pi N$, the magnetic energy per particle is a characteristic energy for cyclotron interactions. A similar analysis shows that the ion energy necessary for resonance with the whistler mode is much larger than the electron energy. Since there will ordinarily be few such highly energetic ions, their contribution to wave growth or damping is neglected.

Depending upon their phase with respect to the wave, resonant electrons will see a wave force of one sign which either secularly accelerates or decelerates them. Net wave growth or damping thus depends upon appropriate velocity gradients which determine whether more gain those lose or vice versa. We will treat only those waves resonant with electrons on the high energy tail, where the number of resonant particles, and therefore the growth rate, is small. Then, by writing $\omega = \omega_R + i\gamma$, where ω_R and γ are real, assuming that $\gamma/\omega_R << 1$, we may estimate the singular velocity integrals in (2.13) using the Dirac relation: $\lim_{\gamma \to 0^+} \frac{1}{v_{\parallel} - \frac{\omega - |\Omega^-|}{k}} = \frac{P}{v_{\parallel} - \frac{\omega - |\Omega^-|}{k}} + i\pi (\text{sign}\, k)\, \delta\left(v_{\parallel} - \frac{\omega - |\Omega^-|}{k}\right)$, where P denotes the principal part. Equating real and imaginary parts of (2.13), dropping terms small in the temperature correction, assuming $n^2 >> 1$, we find that ω_R is again given by (2.17) and the growth rate γ is

$$\gamma = \pi \left| \Omega^- \right| \left(1 - \frac{\omega}{|\Omega^-|} \right)^2 \eta^- (V_R) \left\{ A^- (V_R) - \frac{1}{\frac{|\Omega^-|}{\omega} - 1} \right\} \qquad (2.20)$$

where we have defined

$$\eta^- (V_R) = 2\pi \frac{|\Omega^-| - \omega}{k} \int_0^\infty v_\perp dv_\perp F^-(v_\perp, v_\parallel = V_R)$$

and

$$A^-(V_R) = \left. \frac{\int_0^\infty v_\perp \, dv_\perp \left(v_\parallel \frac{\partial F^-}{\partial v_\perp} - v_\perp \frac{\partial F^-}{\partial v_\parallel} \right) \frac{v_\perp}{v_\parallel}}{2\int_0^\infty v_\perp \, dv_\perp \, F^-} \right|_{v_\parallel = V_R} = \left. \frac{\int_0^\infty v_\perp \, dv_\perp \tan\alpha \, \frac{\partial F^-}{\partial \alpha}}{2\int_0^\infty v_\perp \, dv_\perp \, F^-} \right|_{v_\parallel = V_R}$$

where $\alpha = \tan^{-1}(-V_\perp/V_\parallel)$ is the pitch angle. Since an electron must have a specific parallel velocity to be resonant with a wave of frequency ω, but may have any perpendicular velocity, the stability criterion involves the properties of the distribution function integrated over all perpendicular velocities. This integration path is sketched in Figure 1. When a wide band wave spectrum is excited, a large region of velocity space can interact with waves.

$\eta^-(V_R)$ may be roughly interpreted as the fraction of the total electron distribution in a range $\Delta v_\parallel = (|\Omega^-| - \omega)/k = |V_R|$ about cyclotron resonance. $A^-(V_R)$ is a measure of pitch angle anisotropy. We have deliberately chosen a mixed notation in the definition of A^- to emphasize that anisotropy depends only upon the gradient of the distribution function with respect to pitch angle at constant energy, $\partial F/\partial \alpha$. Since $V_R < 0$, $\partial F^-/\partial \alpha > 0$, implies that the distribution at constant energy increases towards flat pitches. That is, there is more perpendicular than parallel energy. For the special case of a velocity distribution which is a product of Gaussians with different temperatures for perpendicular and parallel velocities, A is independent of V_R and reduces to $A^-(T_\perp, T_\parallel) = (T_\perp - T_\parallel)/T_\parallel$.

Since η^- is always positive, waves are necessarily unstable when

$$A^- > \frac{1}{\frac{|\Omega^-|}{\omega} - 1} \tag{2.21}$$

A sufficient condition for instability for those waves resonant with electrons whose $E_R > B^2/8\pi N$ is simply that $\partial F^-/\partial \alpha$ be positive everywhere. Therefore, any mechanism which flattens the pitch angle of every particle, such as

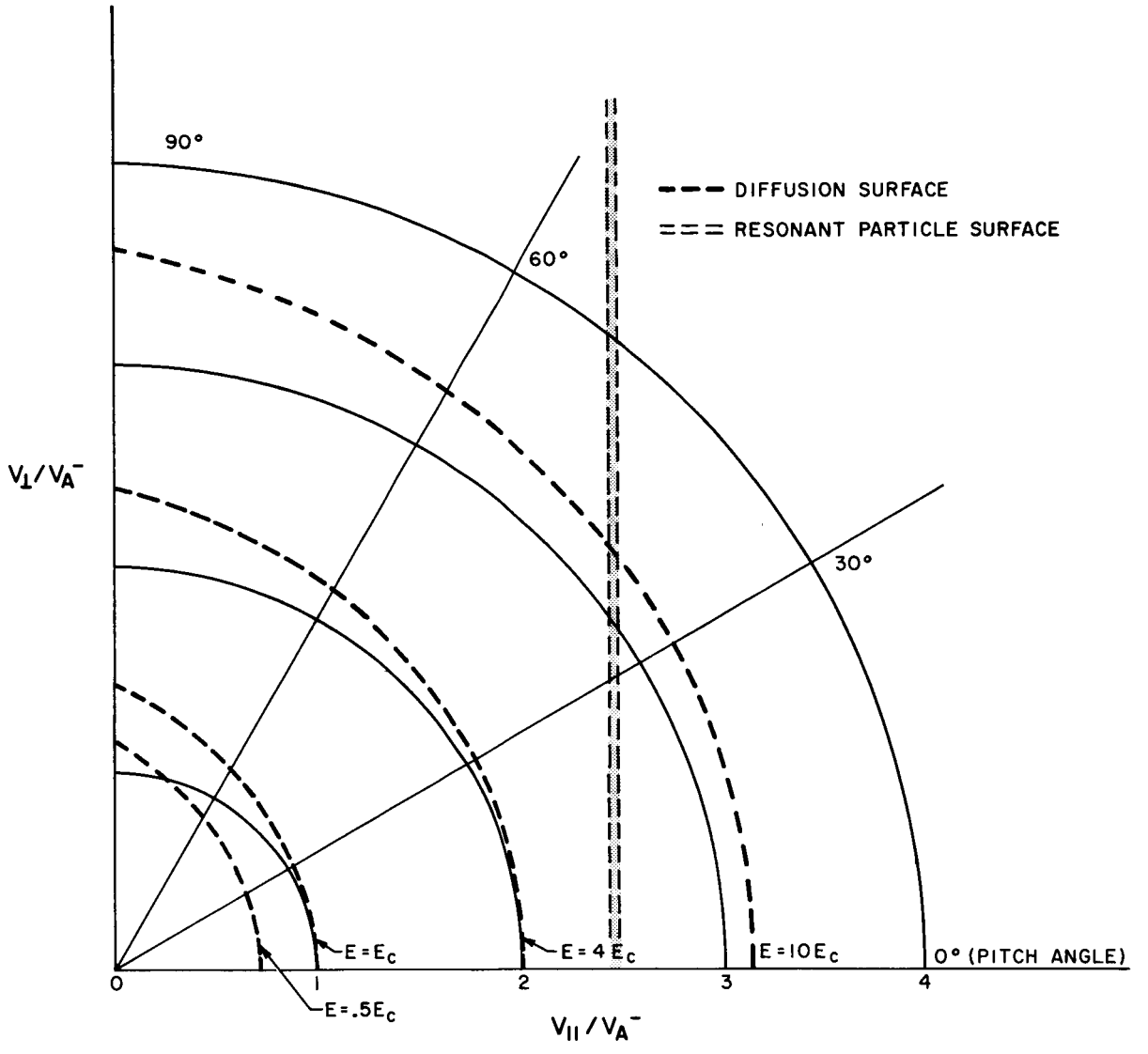

Fig. 1 Intersection of velocity space surfaces for instability and pitch angle diffusion with the plane determined by the $v_\perp$ and $v_{||}$ axes. The stability of waves is determined by the properties of distribution function (Eqs. 2.20 and 2.23) integrated over all particles with a particular parallel velocity (Eqs. 2.18 and 2.24). The solid vertical line indicates the surface in velocity space of importance for stability of a particular wave. Waves of other frequencies interact with a parallel surface at another velocity. The surfaces along which electrons diffuse due to interaction with the whistler mode are also shown. Note that the particle energy on a diffusion surface always decreases towards the $v_{||}$ axis; however, as the energy becomes large compared to $E_c = B^2/8\pi N$ the diffusion surfaces approach constant energy or $|v|$ surfaces.

magnetic field compression, makes the tail of the electron distribution (where $E_R > B^2/8\pi N$) unstable to noise emission in the whistler mode. Similarly, decompression must result in absorption. For this tail, the isotropic state with $\partial F^-/\partial \alpha > 0$ is marginally stable.

In conclusion, whether or not a whistler mode emission is unstable depends only upon the electron pitch angle anisotropy, A^-. Its rate of growth or damping, however, depends upon both the anisotropy A^- and the fraction of electrons which are resonant, η^-.

2.3 The Ion Cyclotron Wave

There is an entirely analogous instability for the ion cyclotron wave for the case of waves propagating parallel to the magnetic field. [Brice, 1965, Jacobs and Watanabe, 1964, Obayashi, 1965, Cornwall, 1965]. The ion cyclotron wave is the anisotropic Alfven mode with left hand circular polarization and frequencies near the ion gyro frequency. In the frequency range, $\omega \approx \Omega^+$, cyclotron interactions with resonant ions become important. For the parallel propagation case, the cold-plasma dispersion relation is

$$n^2 = L \approx \frac{(\omega_p{}^+)^2}{\Omega^+(\Omega^+ - \omega)} \tag{2.22}$$

Ions in cyclotron resonance, with $kV_R = \omega - \Omega^+$, determine stability. The growth rate is found by an analysis similar to that for electrons.

$$\gamma = \frac{\pi\Omega^+}{2}\left(\frac{\Omega^+}{\omega}\right)\frac{(1 - \omega/\Omega^+)^2}{(1 - \omega/2\Omega^+)}\,\eta^+(V_R)\left[A^+(V_R) - \frac{1}{\frac{\Omega^+}{\omega} - 1}\right] \tag{2.23}$$

A^+ and η^+ are defined as in the electron case. Once again, a sufficiently flat pitch angle distribution is unstable.

From (2.9) and the resonance condition, we can express the parallel ion energy necessary for resonance in terms of the wave frequency.

$$E_R = \frac{1}{2} M^+ V_R^2 = E_c \left(\frac{\Omega^+}{\omega}\right)^2 \left(1 - \frac{\omega}{\Omega^+}\right)^3 \tag{2.24}$$

Because of the factor $(\Omega^+/\omega)^2$ appears, the frequency range about the cyclotron frequency for which resonant protons are sufficiently numerous (i.e., have low enough energies) to make significant growth rates will be somewhat narrower than the corresponding electron case. Resonant electrons have much higher energies and may ordinarily be neglected.

2.4 Magnetosonic Mode near Ion Gyroresonance

Near the ion gyro frequency, the real part of the dispersion relation $n^2 = R$ reduces to

$$\frac{c^2 k^2}{\omega^2} = \frac{(\omega_p{}^+)^2}{\Omega^+ (\Omega^+ + \omega)} \tag{2.25}$$

The condition for Doppler shifted ion gyro resonance is $kv_{\parallel} = \omega + \Omega^+$ so that the expression for the resonant ion energy is

$$\frac{E_R}{E_c} = \left(\frac{\Omega^+}{\omega}\right)^2 \left(1 + \frac{\omega}{\Omega^+}\right)^3 \tag{2.26}$$

The growth rate is found by the methods outlined above

$$\gamma = -\frac{\pi \Omega^+}{2} \left(\frac{\Omega^+}{\omega}\right) \frac{(1 + \omega/\Omega^+)^2}{(1 + \omega/2\Omega^+)} \bar{\eta}^+ (V_R) \left\{ A^+(V_R) + \frac{1}{\frac{\Omega^+}{\omega} + 1} \right\} \tag{2.27}$$

where A^+ is defined as before and $\bar{\eta}^+$ is

$$\bar{\eta}^+ (V_R) = 2\pi \left(\frac{\Omega^+ + \omega}{k}\right) \int_0^\infty v_\perp \, d v_\perp \, F^+ \, (v_\perp, \, v_{||} = V_R) \tag{2.28}$$

In contrast with the ion cyclotron wave, the magnetosonic mode is unstable when the pitch angle anisotropy is negative

$$A^+ < - \frac{1}{\frac{\Omega^+}{\omega} + 1} \tag{2.29}$$

For the high energy tail of the proton distribution, there is only a small range of anisotropies of order ω/Ω^+ for which protons are stable to both the ion cyclotron and magnetosonic waves. The trapped proton distribution in the magnetosphere is more likely however, to be unstable to the ion cyclotron wave since diffusion into the loss cones tends to maintain a positive anisotropy.

2.5 Discussion

For the above gyro resonance interactions, the ratio of the parallel energy to the magnetic energy per particle determines the resonant frequency. The velocities corresponding to the critical energy are the electron Alfven velocity $V_A^- = B/\sqrt{4\pi N m^-}$ and the Alfven velocity $V_A^+ = B/\sqrt{4\pi N M^+}$, for the whistler and ion cyclotron modes respectively. If we normalize the wave frequency to the appropriate gyro-frequencies, velocities to the appropriate Alfven velocity and energies to the critical energy, the expressions for phase velocity, group velocity and resonant energies take the simple form outlined in Table 1.

Table 1 Normalized Wave Properties

$$\omega^+ \equiv \omega/\Omega^+ \quad , \quad \omega^- \equiv \omega/|\Omega^-|$$

	Whistler Mode	Ion Cyclotron Mode	Magnetosonic Mode
Phase Velocity	$\frac{V_P}{V_A^-} = [\omega^-(1-\omega^-)]^{1/2}$	$\frac{V_P}{V_A^+} = [1-\omega^+]^{1/2}$	$\frac{V_P}{V_A^+} = [1+\omega^+]^{1/2}$
Group Velocity	$\frac{V_G}{V_A^-} = 2[\omega^-(1-\omega^-)^3]^{1/2}$	$\frac{V_G}{V_A^+} = \frac{[1-\omega^+]^{3/2}}{1-\omega^+/2}$	$\frac{V_G}{V_A^+} = \frac{[1+\omega^+]^{3/2}}{1+\omega^+/2}$
Resonant Velocity	$\frac{V_R}{V_A^-} = \frac{[1-\omega^-]^{3/2}}{[\omega^-]^{1/2}}$	$\frac{V_R}{V_A^+} = \frac{[1-\omega^+)^{3/2}}{\omega^+}$	$\frac{V_R}{V_A^+} = \frac{[1+\omega^+]^{3/2}}{\omega^+}$
Resonant Energy	$\frac{E_R}{E_c} = \frac{[1-\omega^-]^3}{\omega^-}$	$\frac{E_R}{E_c} = \frac{[1-\omega^+]^3}{(\omega^+)^2}$	$\frac{E_R}{E_c} = \frac{[1+\omega^+]^3}{(\omega^+)^2}$

For the tens of kilovolt particle energies observed in the magnetosphere, cyclotron resonance interactions will be most important near the equator on a given line of force. E_c increases rapidly away from the equator and larger anisotropies are needed for local instability of these particles. Moreover, a wave of a given frequency receives its greatest amplitude increment as it crosses the equator on a given line of force. The energy of particles resonant with the wave at each point increase rapidly away from the equator. Since the observed fluxes of energetic particles decrease monotonically with energy and since the total number density increases away from the equator, the fraction η will decrease and the corresponding local growth rates will be smaller. For instance, even though the critical energy at the feet of the lines of force in the ionosphere is again tens of kilovolts and the anisotropy there is large, the total density has increased by perhaps a factor of 10^3, the fraction η has been decreased, and the contribution to the growth will be roughly a thousandth as at the equator. Henceforth, our discussion shall be limited to equatorial cyclotron resonance interactions.

In Figure 2, we plot the magnetic energy per particle at the equator as a function of the equatorial distance L for three local times; midnight, dawn or evening, and noon. We have used total number density measurements summarized by Carpenter and Smith [1964] which are accurate to L = 5; the density has been extrapolated beyond L = 5 using the relation N/B = constant. For the noon magnetic field, we have estimated the distortion of the dipole by the formula

$$B(\text{noon}) \approx \frac{1}{3\,L^3} + 5\cdot 10^{-4}\,(L/10) \qquad (2.30)$$

The dawn (or dusk) field has been assumed undistorted

$$B\ (\text{dawn}) \approx \frac{1}{3\,L^3} \qquad (2.31)$$

while at midnight, the field strength is diminshed because of distortion. There is also a small component due to the field of the tail. [Axford, et al, 1965].

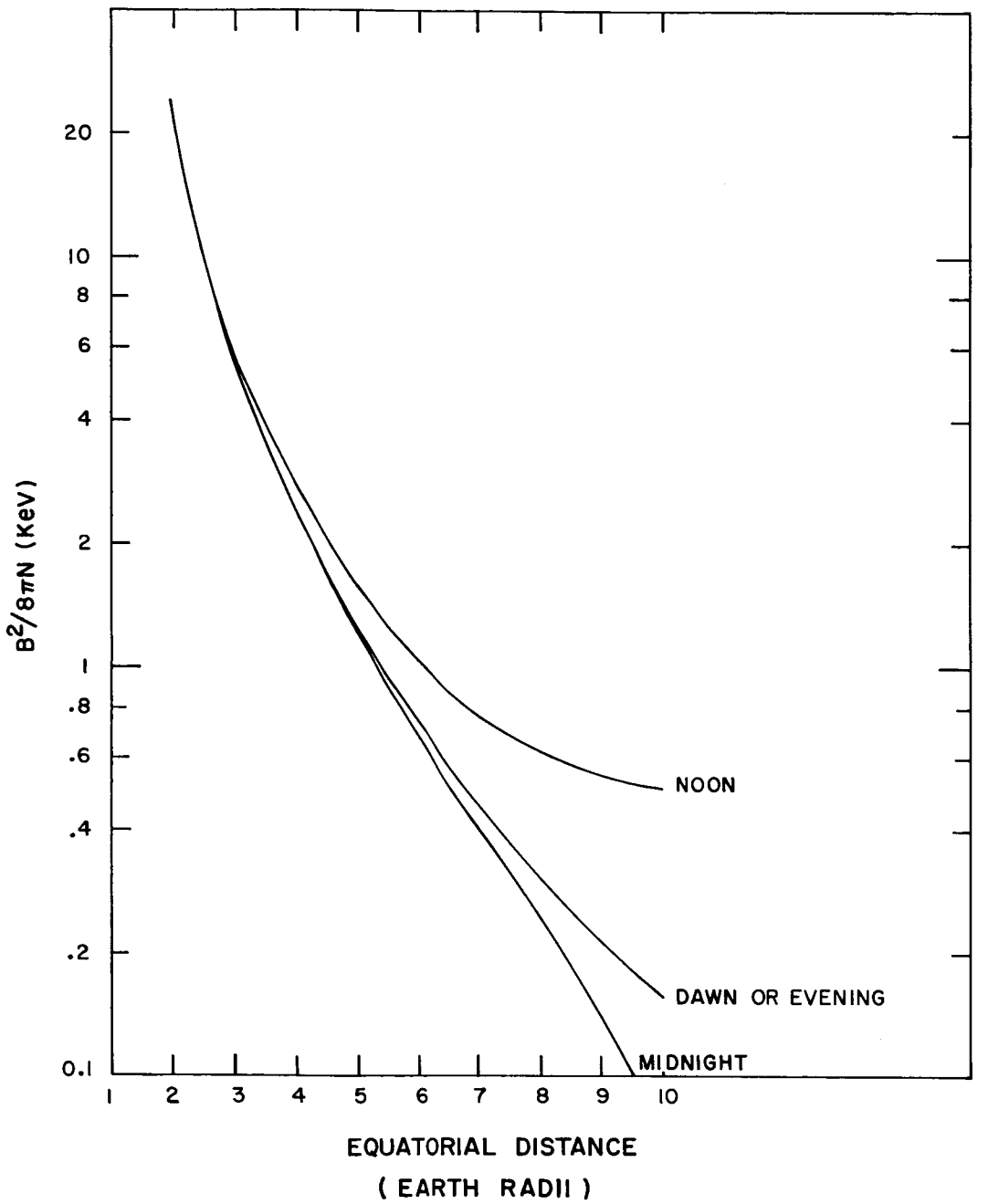

Fig. 2 Magnetic energy per particle at the geomagnetic equator. This plot is based on the idealized magnetic field variation of Eqs. (2.25), (2.26), (2.27) and densities given by Carpenter and Smith (1964). Particles of geophysical interest have an energy by and large well above $B^2/8\pi N$.

$$B\ (\text{midnight}) \approx \frac{1}{3\ L^3} - 2.5 \cdot 10^{-4} \left(\frac{L}{10}\right) + 10^{-4} \qquad (2.32)$$

Knowing the critical energy and the parallel energy of a given particle, we can calculate the phase, group and resonant velocities of the wave resonant with it using Table 1.

These curves are undoubtedly a considerable idealization. Information about the total density beyond $L = 5$ is sparse, and the assumption that N/B is constant is arbitrary. We have not included the sharp "ledge" or decrease in density - which is often observed near $L \approx 3.5$. $B^2/8\pi N$ would have a local maximum near this ledge. Specific numerical estimates based upon these values of $B^2/8\pi N$ may be in error, but we hope that proper qualitative behavior is contained in this description. In any case, the sensitivity of our results to the value of $B^2/8\pi N$ decreases when the particle energy is well above E_c.

2.6 Propagation at an Angle to the Field

For waves propagating at an angle to the magnetic field, stability is determined by the sum of the contributions from resonances corresponding to parallel velocities defined by (see Stix, [1962]).

$$k_{\parallel} V_R\ (m) = \omega - m \Omega^{\pm} \ ; \ m = -\infty \ldots -1, 0, +1, +2, +3, \ldots \qquad (2.33)$$

$k_{\parallel}$ = parallel wave number

Since the wave polarization is elliptical for propagation at an angle to the field, particles can return in phase with the wave after any integral number of Larmor periods, and so the higher cyclotron harmonics produce resonances. In addition, for off angle propagation, there is a component of wave electric field parallel to the external magnetic field which leads to ordinary Landau damping at the so-called Cerenkov resonance ($m = 0$). For the cyclotron harmonics ($m \neq 0$), the sign of the contribution of each

resonance to the growth rate is again given by the anisotropy. Thus compressions will again lead to unstable contributions from these resonances. At the Cerenkov resonance, $m = 0$, $k_{\parallel} v_{\parallel} = \omega$, the energy exchange between particles and waves is analogous to Landau damping; for a distribution which decreases monotonically with energy, this term will give a damping contribution.

The magnitude, and thus, the relative importance of each resonance is given by a coefficient which now depends upon the angle between the wave vector and the field as well as the anisotropy and number of resonant particles at each resonance. For an electron distribution function which decreases monotonically with increasing energy, the largest number of resonant particles will be found at the Cerenkov resonance, since it corresponds to the lowest energy. On the other hand, for small angles to the field, the angular dependence favors the cyclotron $m = -1$ resonance contribution to the growth rate. For strictly parallel propagation, we recall that there is only the $m = -1$ cyclotron resonance and no Cerenkov contribution. As the angle of the wave to the field increases, the relative importance of the usually damping Cerenkov resonance increases. Therefore, parallel propagating waves are the most unstable; the growth rates diminish with increasing angle to the field until at some critical angle θ_c cyclotron growth and Cerenkov damping just balance; beyond θ_c, Cerenkov damping predominates. The harder the energy spectrum (i.e., the more particles at the more energetic cyclotron resonance), the larger θ_c, and hence the more important cyclotron resonance interactions become. For the $1/E^{2-3}$ electron spectrum typically found in the magnetosphere [McDiarmid, et al, 1963], $\theta_c \approx 1$ radian for $A = 1$. Softer spectra correspond to smaller θ_c. Thus if the particle spectrum is hard enough, cyclotron interactions will be important over a significant cone of angles.

Since the parallel waves become unstable most easily, they will be of most interest for pitch angle diffusion. For the remainder of this paper, we will argue in terms of parallel propagating waves, remembering that the actual wave spectrum includes a cone of propagation directions around the parallel whose physical instability mechanism is the same, but whose intensity is smaller.

3. WHISTLER AND ION CYCLOTRON TURBULENCE

3.1 Introduction

The possibility that microscopic turbulence may dominate diffusion and dissipation in plasmas has received considerable attention recently. In this section, we discuss and review the results of a second order turbulence theory, where only effects the order of the square of the wave amplitude are included. After an introductory discussion in 3.1 of the motivation behind this approach to turbulence, we illustrate in 3.2 that second order non-linear wave particle interactions force the particle distribution towards a linear theory marginal stability state. In 3.3 we show that the adjustment to marginal stability is described by diffusion in velocity space at a rate proportional to the square of the wave amplitude. For the whistler and ion cyclotron modes, this amounts to pure pitch angle diffusion. An equation of wave energy transport is discussed in 3.5. Many of these specific formulae have been more formally derived by Chang and Pearlstein [1964] and Andronov and Trakhtengerts [1964].

Fishman, et al, [1960] observed in connection with the theory of collision-free shock waves that plasma turbulence could be more tractable theoretically than aerodynamic turbulence. In contrast with aerodynamic turbulence, which consists of eddies stationary with respect to the fluid, the waves comprising plasma turbulence do propagate and, as a result, high-order correlations do not have time to form. Therefore, the waves have random phases. In addition, plasma waves in many cases can derive energy only from a limited reservoir and cannot grow to large amplitudes. For both these reasons, it is fruitful to view a weakly turbulent plasma as an ensemble of particles and small amplitude collective modes (waves) whose properties are determined in linear theory. Dissipation must then arise from combinations of interactions between particles and waves. Particle-particle interactions or ordinary Coulomb collisions are usually negligible. Turbulent dissipation is created by two distinct non-linear interactions: wave-wave scattering [Sturrock, 1957, Fishman, et al, 1960, Camac, et al, 1962, Kadomtsev and Petviashvili, 1963] and wave-particle interactions [Drummond and Pines, 1962, Vedenov, Velikhov and Sagdeev, 1962]. Wave-wave

scattering is the loss of coherence of a wave propagating in a medium made nonuniform by other waves. Where the waves are almost linear, this amounts to creating sum and difference modes in a binary wave collision. For the present problem, wave-wave scattering is unimportant and we shall not discuss it further except for an a posteriori justification of its neglect (Section 8).

The wave-particle interaction appears even in linear theory, since wave growth or damping depends upon gradients in the velocity distribution at resonance. The non-linear effect is that the wave in turn changes the resonant particle distribution at a rate dependent upon wave energy.

3.2 The Approach to Marginal Stability

To show that non-linear wave-particle interactions modify wave growth to reduce the instability and to force the velocity distribution towards a marginal linear stability state, we will first discuss the change in kinetic energy of a single electron interacting with a whistler. For each wave quantum emitted or absorbed the change in wave energy is $\hbar\omega$. Similarly the change in momentum is $\hbar k$. The change in parallel energy, $dE_{\parallel}$ of the interacting particle is then $-\hbar k V_R$ and the ratio of the total change in particle energy, $dE = -\hbar\omega$, to the change in parallel energy is then

$$\frac{dE}{dE_{\parallel}} = \frac{\omega}{k V_R} \tag{3.1}$$

Using (2.18) this may be rewritten as

$$\frac{dE}{dE_{\parallel}} = -\frac{1}{\frac{|\Omega^{\pm}|}{\omega} - 1} \quad \text{or} \quad \frac{dE_{\perp}}{dE_{\parallel}} = -\frac{1}{1 - \frac{\omega}{|\Omega^{\pm}|}} \tag{3.2}$$

In agreement with the correspondence principle, Planck's constant does not appear in the final result. A more classical derivation of (3.2) can be found, for example in Brice [1964].

If the particle distribution is unstable, so that wave energy increases with time, a majority of resonant particles must lose energy, $dE < 0$. This, however, necessarily implies that $dE_{\parallel} > 0$ for this majority. The anisotropy causing the wave growth is therefore diminished and subsequent wave growth slowed. This must lead to a final state where unstable anisotropies are reduced, linear growth rates are zero, and there is therefore a constant finite wave intensity. The time to reach the marginal stability condition from an initially anisotropic distribution is determined essentially by the initial growth rate. Since the wave energy at first grows exponentially with time, it will be sufficiently intense to reduce the anisotropy after a few e-folding times corresponding to the initial growth rate.

Conversely, if the particle distribution corresponds to a negative growth rate, the waves which drive the distribution back to marginal stability cannot be generated internally by particles. However, should there be an external source of waves, the particles will absorb wave energy from it and their distribution will approach marginal stability. Thus, non-linear effects increase the transparency of the plasma.

Since both initially unstable distributions, which produce their own wave energy, and initially stable distributions in the presence of externally maintained waves approach marginal stability, it is tempting to suggest that weakly turbulent plasmas will always be near marginal stability. If disturbances which distort the velocity distribution act slowly compared with the readjustment back to marginal stability, then the distribution never greatly departs from marginal stability. In complicated physical objects, such as the magnetosphere, one cannot strictly guarantee that the growth rate for every wave will decrease monotonically and smoothly. However, it seems clear that large growth rates cannot be long tolerated.

3.3 Weakly Turbulent Pitch Angle Diffusion

The approach to marginal stability and wave-growth self-limitation is properly described by diffusion of particles in velocity space at a rate proportional to the wave energy. A given particle may either gain or lose energy to a particular wave depending upon its initial phase relative to the wave. Thus waves take particles initially at the same velocity and spread them over a region in velocity space; in other words, diffuse them. When the pitch angle distribution is unstable, diffusion creates a flux from large to small pitch angles, which decreases the net particle energy, increases the wave energy, and reduces the anisotropy. Diffusion and wave growth stops when isotropy is attained.

The ratio of the change in parallel and perpendicular energy for a particle interacting with a wave of a given frequency was given in (3.2). This ratio defines the direction in phase space along which particles will diffuse. Making use of the relation, (2.19), between wave frequency and parallel energy of the resonant electrons, (3.2) may be integrated to give the surfaces along which electrons diffuse. These surfaces are also shown in Figure 1. Except where the parallel energy is less than the critical energy, these diffusion surfaces closely approximate circles, or pure pitch angle diffusion. This is explainable in terms of (2.19) and (3.2). When $E_R \gg E_c$, $\omega/|\Omega^-| \ll 1$ and $dE \approx \omega/|\Omega^-|\, dE_{||}$. In this range, the pitch angle is altered without a significant change in energy. Here the wave magnetic forces dominate the wave electric forces. At the opposite extreme, when $E_R \ll E_c$ and $\omega/|\Omega^-| \approx 1$, electric forces dominate, and the relative change in particle energy is greater than the pitch angle change. Figure 1 indicates that the energy diffusion regime does not become important until $E_R/E_c \approx 1$. Henceforth, we shall consider turbulent diffusion only on surfaces of constant energy, corresponding to the approximation $\omega/|\Omega^-| \ll 1$.

Now we demonstrate in semi-rigorous fashion that resonant interactions with randomly phased whistler mode weak turbulence are described by a pitch angle diffusion equation of the standard form. The wave-particle interaction is a stochastic process in which particles in resonance scatter from a random background of wave fluctuations. If the mean velocity change in a given

encounter is small, the distribution function obeys a Fokker-Planck equation [Chandrasekhar, 1960] which we write immediate in spherical coordinates, since we know that to lowest order in $\omega/|\Omega^-|$ or E_c/E_R, there is only a change in pitch angle $(\Delta\alpha)$, and no change in speed (Δv) or Larmor phase $(\Delta\phi)$.

$$\frac{\partial F^-}{\partial t} = \frac{1}{\sin\alpha}\ \partial/\partial\alpha\ \left\{ -\sin\alpha\ \frac{<\Delta\alpha>}{\Delta t}\ F^- + \sin\alpha\ \partial/\partial\alpha\ (DF^-) \right\}$$

$$D \equiv \frac{<(\Delta\alpha)^2>}{\Delta t} \qquad (3.3)$$

Angular brackets denote an average over the fluctuation spectrum; Δt is the mean time step per wave collision.

The first term, the so-called dynamic friction, appears to dominate in the smallness parameter $\Delta\alpha$. However, to lowest order in $\Delta\alpha$, this term is zero because it is equally probable that electrons decrease as increase their pitch angles, since they are randomly distributed in phase with respect to the waves. However, when $B'(\alpha)$ and Δt are functions of α, electrons scattered in one direction experience a subsequently greater random force than those scattered in the other, and this amounts to non-zero dynamic friction in next order.

$$\frac{<\Delta\alpha>}{\Delta t} \approx 0 + <\Delta\alpha\ \ \frac{\partial}{\partial\alpha}\ (\frac{\Delta\alpha}{\Delta t})> = \frac{\partial D}{\partial\alpha} \qquad (3.4)$$

Here we have used the definition of D given in (3.3). Combining the two terms which are second order in $(\Delta\alpha)$, the stochastic (3.3) reduces to a diffusion equation

$$\frac{\partial F^-}{\partial t} = \frac{1}{\sin\alpha}\ \frac{\partial}{\partial\alpha}\ (D\sin\alpha\ \frac{\partial F^-}{\partial\alpha}) \qquad (3.5)$$

We note in passing for the idealized case of an infinite plasma with no loss of particles or wave energy that one would expect diffusion eventually to reach a steady state with zero flux. (3.5) has only two zero flux, time stationary solutions. The first, when $D = 0$, is the trivial case corresponding to no wave energy present to drive pitch angle diffusion. On the other hand, when there is wave energy so that $D \neq 0$, $\partial F/\partial \alpha = 0$ is time stationary, regardless of any dependence of D upon α. Pitch angle isotropy is just the marginal stability state correspond to the $\omega/|\Omega^-| \ll 1$ approximation. The form of (3.5) therefore demonstrates that when $D \neq 0$ the pitch angle distribution must evolve irreversibly towards a final state of marginal stability to all waves. Since the growth rate is then zero, the wave distribution is also stationary.

3.4 Pitch Angle Diffusion Coefficient as a Function of Wave Energy

Since the amplitude of waves resonant with particles of different velocities parallel to the magnetic field may differ, the scattering rate, and therefore the diffusion coefficient is in general pitch angle dependent. We estimate the change in pitch angle for a given resonant velocity due to interactions with waves in a narrow wave-number band of width Δk about resonance. The relationship $\tan\alpha = -v_\perp/v_\parallel$ implies that $\Delta\alpha \approx -\Delta v_\parallel/v_\perp$. $\Delta v_\parallel$ is given by the net acceleration due to those waves near resonance multiplied by the time a typical particle remains in resonance.

$$\Delta\alpha \approx -\frac{\Delta v_\parallel}{v_\perp} \approx \frac{e v_\perp B'}{m^- c}\,\frac{\Delta t}{v_\perp} = |\Omega^-|\,\frac{B'}{B}\,\Delta t \qquad (3.6)$$

so that

$$D \approx \frac{(\Delta\alpha)^2}{2\Delta t} \approx \frac{(\Omega^-)^2}{2}\left(\frac{B'}{B}\right)^2 \Delta t \qquad (3.7)$$

where B is the ambient magnetic field strength, and B', the wave amplitude near resonance.

The change with time of the relative phase of particle and wave, ϕ, is given by

$$\frac{d\phi}{dt} = kv_{\parallel} - |\Omega^-| \tag{3.8}$$

Δt is roughly the time a particle at distance $\Delta k/2$ out of resonance changes its phase by one radian, or from (3.8) $\Delta t \approx 2/\Delta k v_{\parallel}$. Thus writing $v_{\parallel} = v \cos\alpha$, D becomes

$$D \approx |\Omega^-| \quad \frac{(B')^2/\Delta k}{B^2} \quad \frac{|\Omega^-|}{v|\cos\alpha|} \tag{3.9}$$

In the limit of small Δk, $(B')^2/\Delta k$ is just the energy per unit wave number at resonance, B_k^2. Since $|\Omega^-|/v$ is a typical wave number for the whistler mode spectrum,

$$D \approx \frac{|\Omega^-|}{|\cos\alpha|} k^* \left(\frac{B_k}{B}\right)^2 \equiv \frac{D^*}{|\cos\alpha|} \tag{3.10}$$

$$k^* \equiv \frac{|\Omega^-|}{v}$$

When the wave spectrum is reasonably smooth, $B_k^2 k^*$ is a good estimate of the total wide band wave intensity in the whistler mode. The factor $1/|\cos\alpha|$ has been explicitly retained to illustrate that particles with large parallel velocities on a given velocity shell cross parallel-aligned inhomogeneities more rapidly than those with mostly perpendicular velocity. Provided there is an equal intensity of waves propagating parallel and anti-parallel to the external magnetic field, the diffusion rate in the hemispheres $0 \leq \alpha \leq \pi/2$ and $\pi/2 \leq \alpha \leq \pi$ will be the same.

Entirely similar arguments lead to a diffusion equation of the same form for ions. Here the diffusion coefficient D is roughly $\Omega^+ k^* (B_k/B)^2$,

where $B_k^2 k^*$ is the energy density in ion cyclotron waves. Because the range of frequencies in ion cyclotron resonance with particles is narrow, the assumption $\omega/\Omega^+ << 1$ corresponding to pure pitch angle diffusion is more restrictive.

3.5 Wave Dynamics

So far, there has been no attempt to account for the wave energy which is created and absorbed in cyclotron interactions and which determines the rate of pitch angle diffusion. Wave energy density can change by growth or damping in resonant interactions, and by spatial transport at the group velocity. The fact that waves can propagate out of finite systems can be of critical importance. We make a closed set of equations by writing the appropriate equation for wave energy transport, noting that resonant interactions are adequately described by the linear growth rate γ_k.

$$(\partial/\partial t + \underset{\sim}{V}_G \cdot \underset{\sim}{\nabla}) B_k^2 = 2\gamma_k B_k^2 \qquad (3.11)$$

$\underset{\sim}{V}_G(k)$ is the group velocity and γ_k is the growth rate appropriate to a mode with wave number k computed at any instant.

3.6 Summary

Second order non-linear wave-particle interactions tend on the average to reduce the absolute magnitude of the linear growth rates computed from the velocity distribution. Since gradients in velocity space determine the growth rate, the reduction in growth rate is a velocity space diffusion process whose rate is fixed by the wave energy. To a good approximation, whistler and ion cyclotron mode radiation drive diffusion purely in pitch angle. The diffusion tends to force the particle distribution toward marginal stability.

4. STEADY STATE DIFFUSION INTO A LOSS CONE: "DRIZZLE"

4.1 Introduction

Weak whistler and ion cyclotron turbulence clearly are promising candidates for the explanation of the observed particle precipitation. In Section 2 and 3 we developed the conceptual framework and mathematical apparatus necessary to understand pitch angle scattering. To apply this understanding to the real physical problem, we develop in this section specialized solutions of the diffusion equation relevant to the magnetospheric plasma. In Sections 5, 6, 7 and 8 we shall finally test these ideas by comparison with observations.

When the plasma is finite, so that both waves and particles can escape from the system, the concept of the approach to marginal stability must be replaced by that of steady state diffusion equilibrium. The underlying mechanism is the same in both cases. Unacceptably large growth rates are reduced by the ensuing enhanced pitch angle diffusion. However, without replenishment of particles and waves in a finite plasma, the whole process would die out. With replenishment, a steady state is conceivable.

It is clear that escaping wave energy can be replaced by generation from an unstable particle distribution if the growth rate is positive and sufficiently large, in other words, if the medium has gain. Suppose that whistler and ion cyclotron mode radiation bounces back and forth along a tube of force between points which may reflect imperfectly. Then the condition that the wave intensity remain constant is

$$e^{\gamma T_w} = \frac{1}{R} \quad \text{or} \quad \gamma = \frac{1}{T_w} \ln 1/R \equiv \nu \tag{4.1}$$

where R is the reflection coefficient, γ, is a mean growth rate, typically the equatorial value for reasons cited in Section 2, and T_w is the group delay time, or one wave packet bounce period. Since R enters only logarithmically, γ must be only a few times the basic frequency $1/T_w$ to maintain wave equilibrium.

This only deflects the question back to the particle distribution. What keeps the growth rate positive when left to its own devices it would revert to zero? For it to be positive at all, a flat pitch angle distribution must be maintained. There must be sources of pitch angle anisotropy - macroscopic mechanisms which steadily flatten the pitch angle distribution or add particles preferentially with flat pitches. Not only must the growth rate be positive, but it must also have the proper magnitude to satisfy (4.1). Since steady diffusion sends particles towards the loss cone where they are lost, particles must clearly be replaced. Therefore there must be local acceleration mechanisms. To our knowledge, no entirely satisfactory acceleration mechanism has been proposed. However, assuming that anisotropy and acceleration mechanisms exist, we can discuss the diffusion equilibrium which must ensue.

4.2 Diffusion Solution Including a Loss Cone

Three basic physical time scales, the wave escape time T_w, the particle escape time T_E, and the particle lifetime T_L, parametrize the magnetospheric diffusion equilibrium. We shall approximate T_w, which has already been defined, by

$$T_w \approx \frac{L R_E}{V_G} \tag{4.2}$$

where $R_E = 6.4 \times 10^8$ cm, L is the equatorial distance in Earth radii, and V_G is the equatorial group velocity.

Once a particle has been scattered into the loss cone at the equator, it remains in the diffusion region a time T_E before it is lost to the atmosphere. The escape time T_E is roughly the quarter-bounce time.

$$T_E \approx \frac{L R_E}{V_R} \tag{4.3}$$

A flat pitch angle particle diffuses to the loss cone in roughly one lifetime T_L. A more precise definition of T_L is the total number of trapped particles on a tube of force divided by the rate they diffuse into the loss cone.

In this section we solve formally for the pitch angle distribution in diffusion equilibrium to find both the number of trapped particles and the loss rate - and therefore the lifetime - in terms of the equatorial wave intensity and the escape time T_E. The equilibrium pitch angle anisotropy thereby is fixed. In consequence, we shall be able to show in Section 5 that T_w sets an upper limit to stably trapped intensities.

We first find the solution inside the loss cone, and then match this at the loss cone boundary to the appropriate solution outside. Particles in the loss cone will be lost from the tube of force in a time comparable with T_E. We estimate this sink by a term of the form F/T_E. The diffusion equation within the loss cone $\alpha < \alpha_o$, is therefore

$$1/\alpha \; \partial/\partial \alpha \; (D^* \alpha \frac{\partial F}{\partial \alpha}) - \frac{F}{T_E} = 0 \qquad (4.4)$$

assuming $\alpha_o << 1_o$.

If $B^2_k k^*$ is assumed constant, corresponding to a wave spectrum independent of frequency, the solution to (4.4) which is finite at $\alpha = 0$ is

$$F = X(v) \, I_o\left(\frac{\alpha}{\sqrt{D^* T_E}}\right) \qquad (4.5)$$

where $X(v)$ is an arbitrary function and I_o is the modified Bessel function. X will be fixed by matching at $\alpha = \alpha_o$ with the solution outside the loss cone.

We must assume an undetermined particle source outside the loss cone which maintains a steady state. The diffusion equation for this region is therefore

$$\frac{1}{\sin \alpha} \frac{\partial}{\partial \alpha} (D \sin \alpha \frac{\partial F}{\partial \alpha}) = s(\alpha, v) \; ; v^2 = v_\perp^2 + v_{11}^2 \qquad (4.6)$$

where $s(\alpha)$ represents the addition to a given energy shell of new particles at flat pitches to maintain the loss flux. If we assume for simplicity that all particles are injected at flat pitches (so that $s(\alpha) = 0$ except at $\alpha = \pi/2$),

the diffusion flux is constant at any angle $\alpha < \pi/2$ and equal to S.

$$D^* \tan\alpha \frac{\partial F}{\partial \alpha} = \int_0^{\pi/2} d\alpha \sin\alpha \delta(\alpha - \pi/2) s(\alpha, v) = S(v) \tag{4.7}$$

S is also the rate that particles enter the loss cone and is therefore the precipation flux. Assuming that $B_k^2 k^*$ is constant, we integrate (4.7) once more to find F

$$F = \frac{S(v)}{D^*} \ln(\sin\alpha) + Z(v) \tag{4.8}$$

where Z is an arbitrary constant, and $D^*/\cos\alpha = D$. Matching the solutions inside and outside the loss cones (4.5) and (4.7) by requiring that F and the diffusion flux be continuous, gives two conditions which eliminate X and Z. (4.8) becomes after matching

$$F(\alpha, v) = F_2(\alpha, v) = \frac{S(v)}{D^*} \left\{ h(\alpha_o) + \ln \frac{\sin\alpha}{\sin\alpha_o} \right\} ; \quad \alpha_o < \alpha < \pi/2 \tag{4.9}$$

where $h(\alpha_o)$ is the loss cone solution (see (4.10)) evaluated at the boundary $\alpha = \alpha_o$.

$$F_1(\alpha, v) = \frac{S(v)}{D^*} h(\alpha) = \frac{S(v)}{D^*} \left\{ \frac{\sqrt{D^* T_E}}{a_o} \frac{I_o(\alpha/\sqrt{D^* T_E})}{I_1(a_o/\sqrt{D^* T_E})} \right\} \tag{4.10}$$

Thus, knowing the loss rate, T_E, a_o, and D^* we can calculate the corresponding equilibrium pitch angle distribution. (The above solutions are, of course, symmetric about $\alpha = \pi/2$.)

For pure pitch angle diffusion, the lifetime is the total number of trapped particles on a given energy shell divided by the loss rate.

$$T_L = \frac{1}{D^*} \int_{\alpha_o}^{\pi/2} d\alpha \sin\alpha \left\{ h(\alpha_o) + \ln \frac{\sin\alpha}{\sin\alpha_o} \right\}$$

$$\approx \frac{1}{D^*} \left\{ h(\alpha_o) - \ln \left(e \tan \frac{\alpha_o}{2} \right) \right\} \qquad (4.11)$$

The diffusion strength is parametrized by

$$z_o = \alpha_o / \sqrt{D^* T_E}$$

The pitch angle profiles observed in the loss cone by [O'Brien, 1964] vary from quite steep to nearly isotropic. These correspond to "weak" and "strong" diffusion, in two limits of the parameter z_o. In weak diffusion, there are many more particles at the edge of the loss cone ($\alpha \approx \alpha_o$) than at the center, $\alpha = 0$, and many more still at flat pitches $\alpha = \pi/2$ than near the loss cone. In this limit, $z_o \gg 1$, and the loss cone distribution increases exponentially from $\alpha = 0$ to $\alpha = \alpha_o$ according to the asymptotic representation of the Bessel functions. Here

$$T_L \approx \frac{1}{D^*} \ln (2/e\alpha_o) \qquad (4.12)$$

when $\alpha_o \ll 1$. In this regime, the lifetime depends primarily on wave intensity and only logarithmically on the size of the loss cone.

At the opposite extreme, the wave intensity may sometimes be sufficiently intense to keep the pitch angle distribution nearly isotropic <u>even</u> in the loss cone. The rate of particle precipitation can then depend only upon the size of the loss cone. Therefore, even when diffusion is very strong, there is a minimum allowable lifetime in steady state, T_L^*, which is independent of the details of wave intensity. Taking $z_o \ll 1$ in the Bessel

functions gives

$$T_L^* \approx \frac{2T_E}{a_o^2} \approx 4\, T_E\, L^3 \tag{4.13}$$

4.3 Special Moments of the Diffusion Equilibrium Distribution

For weak diffusion ($h(a_o) \ll 1$) the above distribution in pitch angle is independent of the particle source strength, the diffusion coefficient or the number of particles. S/D^* appears only as a multiplying constant, and does not determine the functional dependence on a. As a result, the anisotropy, A, is independent of the above parameters. We have made a rather arbitrary choice in assuming that the source of particles, S, is concentrated at $a = \pi/2$. We would, however, not expect order of magnitude changes from other choices of source distributions.

If we specify the particle energy distribution, we can calculate A and η for diffusion equilibrium. In addition, we can relate η, to the omnidirectional flux, J, which is an observed quantity. Assuming the total distribution has the form $N F(a) S(v)/D^*$ where N is the number density and

$$\frac{S(v)}{D^*} = \frac{Q}{(v_\perp^2 + v_{||}^2)^n} \; ; Q = \text{normalizing constant} \tag{4.14}$$

and using (4.9) and (4.10) for $F(a)$, we may calculate the moments η and A for the weak diffusion case. We also drop terms higher order in a_o.

$$\eta \approx \int_{a_o V_R}^{\infty} v_\perp \, dv_\perp \; 2\pi\Omega \; V_R \frac{S(v)}{D^*} \ln\left(\frac{\sin a}{\sin a_o}\right)$$

$$\approx \frac{2\pi V_R^3}{(2n-2)} \frac{S(V_R)}{D^*} \left\{ \ln\left(\frac{1}{a_o}\right) + 0(1) \right\} \tag{4.15}$$

$$A \approx \frac{1}{2\left\{\ln(1/a_o) + 0(1)\right\}} \tag{4.16}$$

Thus for auroral field lines, $A \approx 1/6$.

The accurate value of A is not crucial in further discussions. However, the idea that in diffusion equilibrium A will be a constant somewhat less than unity is most important. This suggests that unacceptably large growth rates cannot be reduced by isotropization in pitch angle alone, but that resonant particles must be lost as well. In effect it is impossible to have a very small A and a very large η and be in equilibrium to all wave modes. This conclusion shall be used in Sections 5 and 6 to determine the upper limit on stably trapped particle intensities.

Since the fraction of particles near resonance, η, can play a crucial role, it is important to relate η to the quantity $J/V_R N$ (which has the same dimensions as η) since J, the omnidirectional flux, N the total number density and the resonant velocity V_R are observables. Using the distribution (4.14), we compute the moment $J/V_R N$ in the weak diffusion limit and compare with $\eta(V_R)$.

$$\frac{J(>E_R)}{V_R N \eta} \approx \frac{4\pi Q}{V_R \eta} \int_{V_R}^{\infty} \frac{v^3 dv}{v^{2n}} \int_{\alpha_o}^{\pi/2} F_2(\alpha, v) \sin\alpha \, d\alpha$$

$$\approx 2\left(\frac{n-1}{n-2}\right) \frac{\ln(2/e\alpha_o)}{\ln(1/\alpha_o)} \approx 2 \qquad (4.17)$$

Thus, the two moments η and J are simply related by the appropriate dimensional constants and a numerical factor of order unity. This numerical factor is essentially independent of both the energy spectrum and the size of the loss cone.

5. WHISTLER MODE UPPER LIMIT TO STABLY TRAPPED ELECTRON FLUX

5.1 Introduction

It was shown in Section 4 that the pitch angle anisotropy A in steady state weak diffusion is virtually a constant. This led to the suggestion that the whistler mode growth rate must approach its steady state value by precipitating resonant electrons. To maintain a steady state, there must be an electron acceleration source which continually creates new resonant particles. The

rate at which this occurs determines the lifetime and the magnitude of the precipitation flux. However, the actual maximum omnidirectional flux which can be stably trapped is independent of the acceleration rate. Resonant electrons accumulate due to acceleration until their intensity is sufficient to cause self-excited pitch angle diffusion. Further acceleration then only results in precipitation, and the trapped flux cannot increase. This limiting electron flux is calculated and compared with observations in this section. The observed electrons > 40 keV are found to be close to their whistler self-excitation limit, with correspondingly heavy precipitation, for the range $L > 4$.

5.2 Calculation of Limiting Electron Flux

The maximum stably trapped flux, J^*, will be implicitly given by equating the wave growth rate to the wave escape rate

$$\gamma \approx \frac{\ln G}{T_w} \tag{5.1}$$

since γ involves the moment η which can be related to an omnidirectional flux J. G is the gain on one wave traversal of the active region of a tube of force necessary to balance wave absorption and/or losses. G must be essentially equal to $1/R$, the reflection coefficient discussed in Section 4.1. A factor of 10 in $\ln G$ corresponds to 2×10^4 in wave amplitude, 4×10^8 in wave energy. While the detailed physical properties which determine G are not well known, it is clear that γ cannot be more than a few times the wave-escape frequency $1/T_w$.

Using the expression (2.20) for the growth rate, (4.2) for T_w, Table 1 for the group velocity, and (4.17) for the omnidirectional flux, we solve (5.1) for J^* $(> E_R)$.

$$J^*(>E_R) \approx \frac{(1 - \frac{\omega}{|\Omega^-|})(\frac{c}{\pi^2 e R_E})}{A^- - \frac{1}{\frac{|\Omega^-|}{\omega} - 1}} \quad \frac{B \ln G}{\ell} \ / \mathrm{cm}^2\text{-sec.} \tag{5.2}$$

where ℓ is the effective length of the line of force in Earth radii (roughly the equatorial distance of the line of force), B the equatorial magnetic field strength in Gauss, $R_E = 6.4 \times 10^8$ cm, and Earth radius, $c = 3 \times 10^{10}$ cm/sec, the speed of light, and $e = 5 \times 10^{-10}$ esu, the electronic charge. A^- is the anisotropy in diffusion equilibrium, typically 1/6. When the $\omega/|\Omega^-| \ll 1$ approximation is valid, so that $\omega/|\Omega^-| \approx E_c/E_R$, (5.2) reduces to

$$J^*(>E_R) = \frac{(1 - E_c/E_R)}{(A^- - E_c/E_R)} \; 10^{10} \; \frac{B \ln G}{\ell} \; / \text{cm}^2\text{-sec.} \qquad (5.3)$$

We first examine the energy dependence of J^* implied by 5.3. At the low energy end of the spectrum, when $E_c/E_R \approx A^- \approx 1/6$. J^* is singular and becomes negative at lower energies. However, this singularity occurs when the $\omega/|\Omega^-| \ll 1$ approximation begins to break down, and may not be real. A more accurate calculation is needed to clear up this point.

In addition $J^*(> E_R)$ is independent of energy at high energies. In other words, the limiting spectrum is flat. Since the actual spectrum cannot be flat to arbitrarily large energies, there must be a transition energy above which the trapped electron intensity has not reached its self-excitation limit. Above the transition energy, electrons do not have sufficient gain to precipitate, and below it, they can precipitate when there are acceleration sources. Such a transition with increasing electron energy from a diffusion dominated to a stably trapped regime is necessary to explain the fact that very high energy electron precipitation ($E > 1.6$ meV), if it occurs, is unrelated to that at lower energies [O'Brien, 1964]. Above the transition energy, the observed electron integral energy spectra will be fixed by the acceleration mechanism, while below it should be reasonably flat. It is important to note that the limiting flux criterion allows hard energy spectra for the trapped electron population and is not inconsistent with the observations of $1/E^{1-2}$ spectra [McDiarmid, et al, 1964].

If electrons are continuously accelerated, their trapped flux will eventually be limited by whistler mode pitch angle diffusion. The flux at which they are limited does not depend upon the rate of particle acceleration. Therefore, in those regions where acceleration is continuous, the observed fluxes should be consistently near critical, with intensity variations which depend only upon changes in the microscopic properties of the plasma, B, ℓ, E_c and so on. Whenever observed fluxes are well below their limit, there can of course be intensity variations which depend upon the acceleration mechanism. Thus, the trapped electron population will most clearly respond to the acceleration mechanism at low L-shells, where critical fluxes are high, and at high particle energies, because high energy particles are less often near flux-limiting instability.

When acceleration is continuous, more and more of the electron distribution reaches the limiting flux and the transition energy therefore increases with time. Thus, observed trapped particle energy spectra should become progressively harder with time. For instance, when acceleration is enhanced, high energy electrons should have their peak after the low energy electron fluxes. This is somewhat reminiscent of behavior described by Freeman [1964] for magnetic storms and for variations with K_p.

In the comparison of J^* (> 40 keV) with the corresponding observed electron fluxes, we may neglect E_c/E_R. This assumption makes an error of a factor two at $L \approx 3$ and a progressively smaller error at larger L-shells. From the analysis of Section 4 we take $A^- \approx 1/6$. For the magnetic field strength B we substitute (2.25), (2.26), and (2.27). We assume the effective length of the line of force has no diurnal variation and we estimate $\ln G/\ell$ by 3/L, where L is the equatorial distance of the tube of force in Earth radii. The results estimated for J^* are probably accurate to a factor three.

$$J^*(\text{noon}, > 40\ \text{keV}) \approx \frac{7 \times 10^{10}}{L^4} + 10^6 \ (/\text{cm}^2\text{-sec})$$

$$J^*(\text{dawn, evening}, > 40\ \text{keV}) \approx \frac{7 \times 10^{10}}{L^4} \ (/\text{cm}^2\text{-sec}) \qquad (5.4)$$

$$J^*(\text{midnight}, > 40\ \text{keV}) \quad \frac{7 \times 10^{10}}{L^4} + \frac{2 \times 10^7}{L} - 5 \times 10^6 \ (/\text{cm}^2/\text{sec})$$

In Figure 3 we plot J^* (> 40 keV) calculated in the above way as a function of radial distance and for three local times; midnight, dawn or evening, and noon. Superposed is the range, minimum to maximum, of > 40 keV electron fluxes observed near the equatorial plane by Explorer XIV over a period of months [Frank, Van Allen and Hills, 1964; Frank, 1965] and also the average distribution with L-shell of > 40 keV precipitated electrons observed on Injun III [O'Brien, 1964]. The highest equatorial fluxes observed lie quite near the calculated upper limits at each radial distance. Moreover, the observed equatorial fluxes were always well below critical for $L < 4$, and there was little precipitation. On the other hand, for $L > 4$, the equatorial fluxes were often critical, and there is considerable precipitation. Thus, we conclude that the latitude distribution of precipitation and equatorial trapped intensities are mutually consistent.

In Figure 4, we compare the theoretical flux limit for $L = 5, 6, 8, 10$ with the actual distribution of fluxes measured near the equatorial plane on Explorer XIV. Although occasional points violate the limit, the large majority lie in the region below the limit. At $L = 5$, when the observed electron fluxes are ordinarily less than J^* (> 40 keV), there is a reasonable scatter of points corresponding presumably to a dependence upon the acceleration mechanism. At $L = 6$, the observed fluxes cluster quite closely about J^* with a smaller scatter than at $L = 5$. At $L = 8$ and 10 the scatter again increases, but here it may well be due to time changes in the magnetic field strength, length of the line of force, and so on, which would be far more pronounced than at $L = 5$ and 6. One would particularly expect the night side to be strongly affected by variation in the solar wind and the magnetospheric tail flow. The behavior at $L = 6$ in particular and less clearly at $L = 8$ and 10, suggests that a continuous acceleration mechanism exists for $L \geq 6$ which maintains the trapped electron intensity near its self-excitation limit.

Since the Explorer XIV observations extended over some months, many local times were sampled. The data shows some diurnal intensity variations which appears to be consistent with the predicted variation given by (5.4). There is also some evidence from Figure 5.4 that observed 40 keV electron fluxes are closer to the critical level on the morning side of the Earth than at

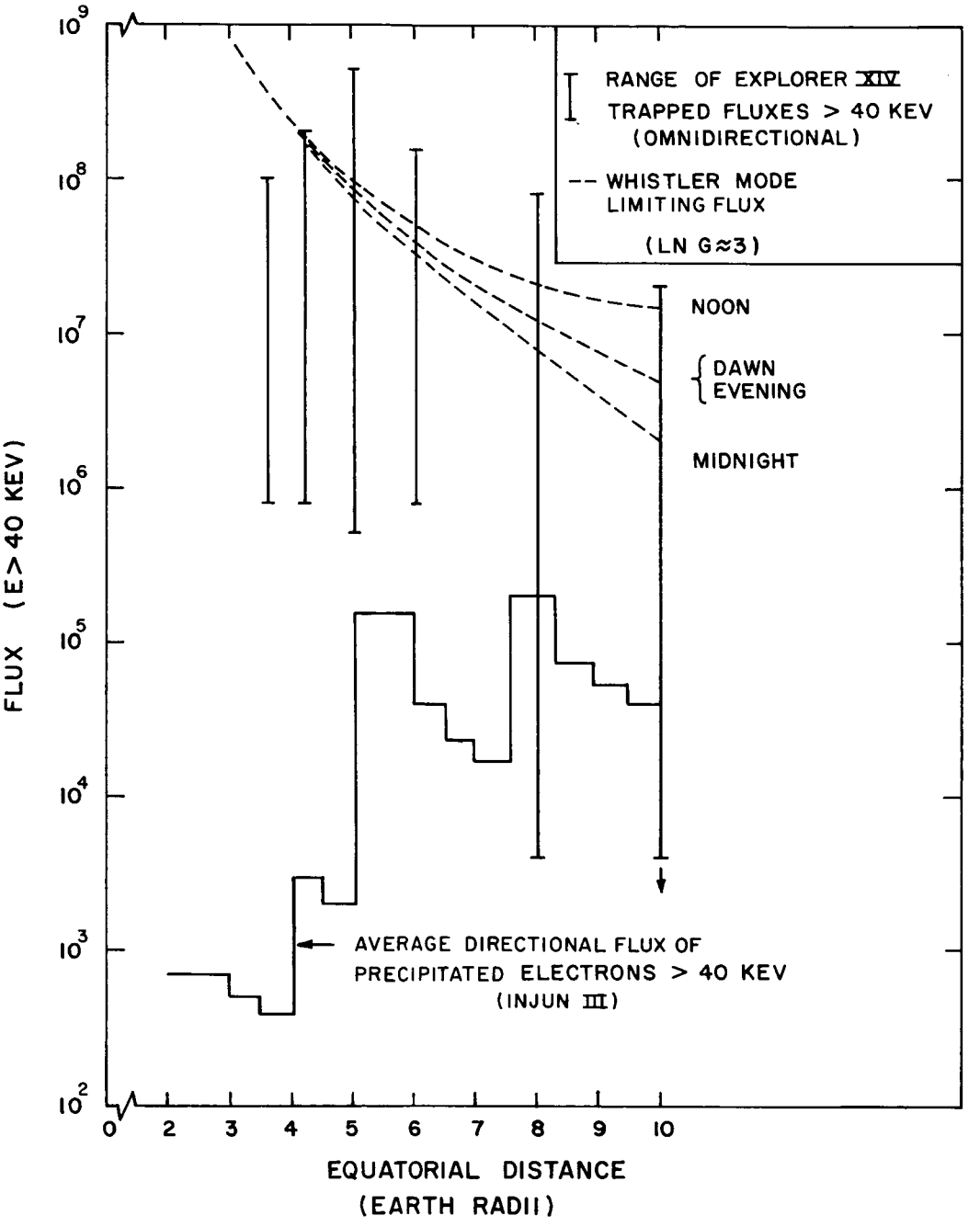

Fig. 3 Limitation on trapped > 40 keV electron fluxes. The theoretical limiting flux J^* is compared with Explorer XIV equatorial trapped fluxes as a function of the equatorial radial distance. The largest observed trapped fluxes are indeed close to the theoretical upper limit. We also show the distribution with L-shell of Injun III precipitated electrons. As expected, strong precipitation only occurs where trapped fluxes can be comparable with the calculated limiting flux.

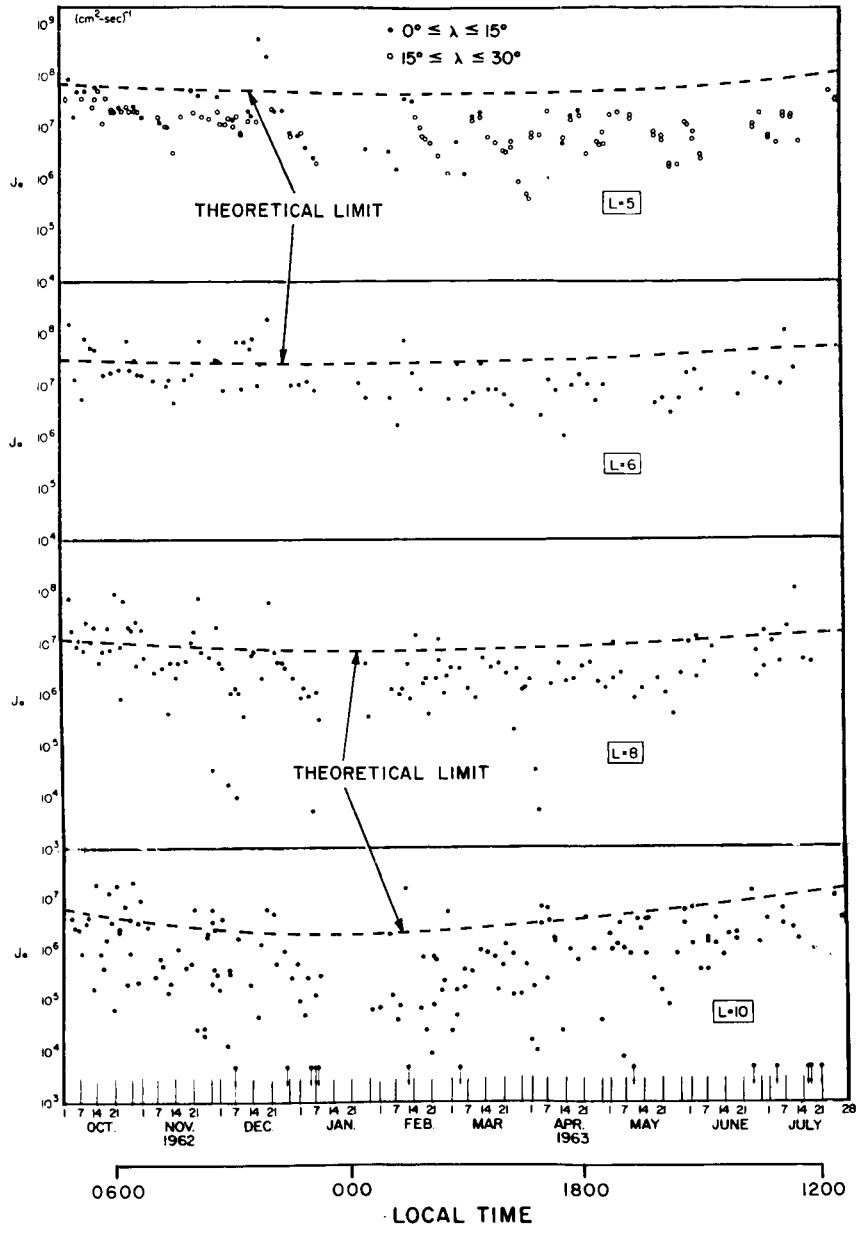

Fig. 4 Limitation on trapped electrons > 40 keV . This diagram permits an estimate of the degree to which observed particle fluxes approach their limiting value. We have superposed the calculated J^* on Explorer XIV data published by Frank (1965). The majority of points are clearly below the predicted limit. The small scatter of points near but below the limit at L = 6 suggests that a continuous acceleration mechanism is operative here.

other local times. This would be consistent with a morning precipitation maximum. Such a maximum has been observed with satellites [McDiarmid and Burrows, 1964] and by riometer absorption techniques [Hartz, Montbriand and Vogan, 1963].

6. LIMITATION UPON TRAPPED PROTON INTENSITIES

The limiting proton flux based on the ion cyclotron instability is found in precisely the same way as for electrons. Thus

$$J^*(>E_R) \approx \frac{(1-\frac{\omega}{\Omega^+})}{\left(A^+ - \frac{1}{\frac{\Omega^+}{\omega}-1}\right)} \frac{c}{\pi^2 e\, R_E} \frac{B \ln G}{\ell} \qquad (6.1)$$

When $E_c/E_R \ll 1$, then $\omega/\Omega^+ \approx \sqrt{E_c/E_R}$ so that (6.1) reduces to

$$J^*(>E_R) \approx \frac{(1-\sqrt{E_c/E_R})}{(A^+ - \sqrt{E_c/E_R})} 10^{10} \frac{B \ln G}{\ell} (/cm^2\text{-sec}) \qquad (6.2)$$

When $\sqrt{E_c/E_R} \ll 1$, the limiting electron and proton fluxes are identical. Therefore the number density of trapped energetic protons can be as much as forty times larger than the density of electrons at the same energy.

The limiting intensity > 120 keV protons corresponding to self-excitation of ion cyclotron waves is plotted in Figure 5. Since $\sqrt{E_c/E_R}$ for these protons becomes roughly 1/10 at $L \approx 4$, this calculation becomes sensitive to the denominator in (6.2) ($A^+ \approx 1/6$) and significant errors may occur at low L-shells. Superposed are a number of radial distributions referred to the equatorial plane of protons with energies between 120 keV and 4.5 meV observed with Explorer XII [Davis and Williamson, 1962]. We have multiplied the directional intensities given by Davis and Williamson [1962] by a factor 4π to translate to the omnidirectional intensities shown

in Figure 5. This procedure is probably as accurate as the calculation of the limiting flux. While the data shown only covers a period of a month, the closeness of the observed fluxes to the limiting flux could imply an acceleration mechanism which is balanced by precipitation beyond L = 4. Since Davis and Williamson, [1962] found relatively soft proton energy spectra, most of the protons observed must have been near the detector threshold of 120 keV. More recently, Davis, Hoffman and Williamson, [1964] have indicated that the intensities of observed 100 keV protons are relatively stable with time, while 1 meV protons exhibit larger time variations. This is consistent with the idea that 1 meV protons usually lie above the transition energy, (i.e., are well below the limiting flux) do not have sufficient intensity to be unstable, and therefore reflect the changes in the acceleration mechanism. Moreover, the constancy with time of > 120 keV protons further strengthens the idea that these protons are maintained at their limiting flux.

7. CONSISTENCY OF LIFETIME AND OBSERVED PITCH ANGLE PROFILES

The satellite Injun III has obtained the distribution with pitch angle of the fluxes of electrons >40 keV near the Earth. We use this data to infer an empirical diffusion coefficient which corresponds to a lifetime in agreement with other independent estimates. It is not possible to predict this lifetime without knowledge of the acceleration sources, but we can state that the lifetimes and observed pitch angle profiles are mutually consistent, thereby strengthening the diffusion hypothesis.

To form a correspondence between Injun III pitch angle data and diffusion theory, we assume that cyclotron resonance interactions occur only in a narrow structureless interaction region in the geomagnetic equatorial plane. To translate data collected by Injun III at 1000 km altitudes to the appropriate equatorial values, we assume the electrons travel adiabatically outside the interaction region. Secondly we assume that the functional dependence upon pitch angle of the flux >40 keV at 1000 km, which is what O'Brien, [1964] observes, is similar to that of the equatorial distribution function itself in the following sense. The equatorial pitch angle distribution should be given

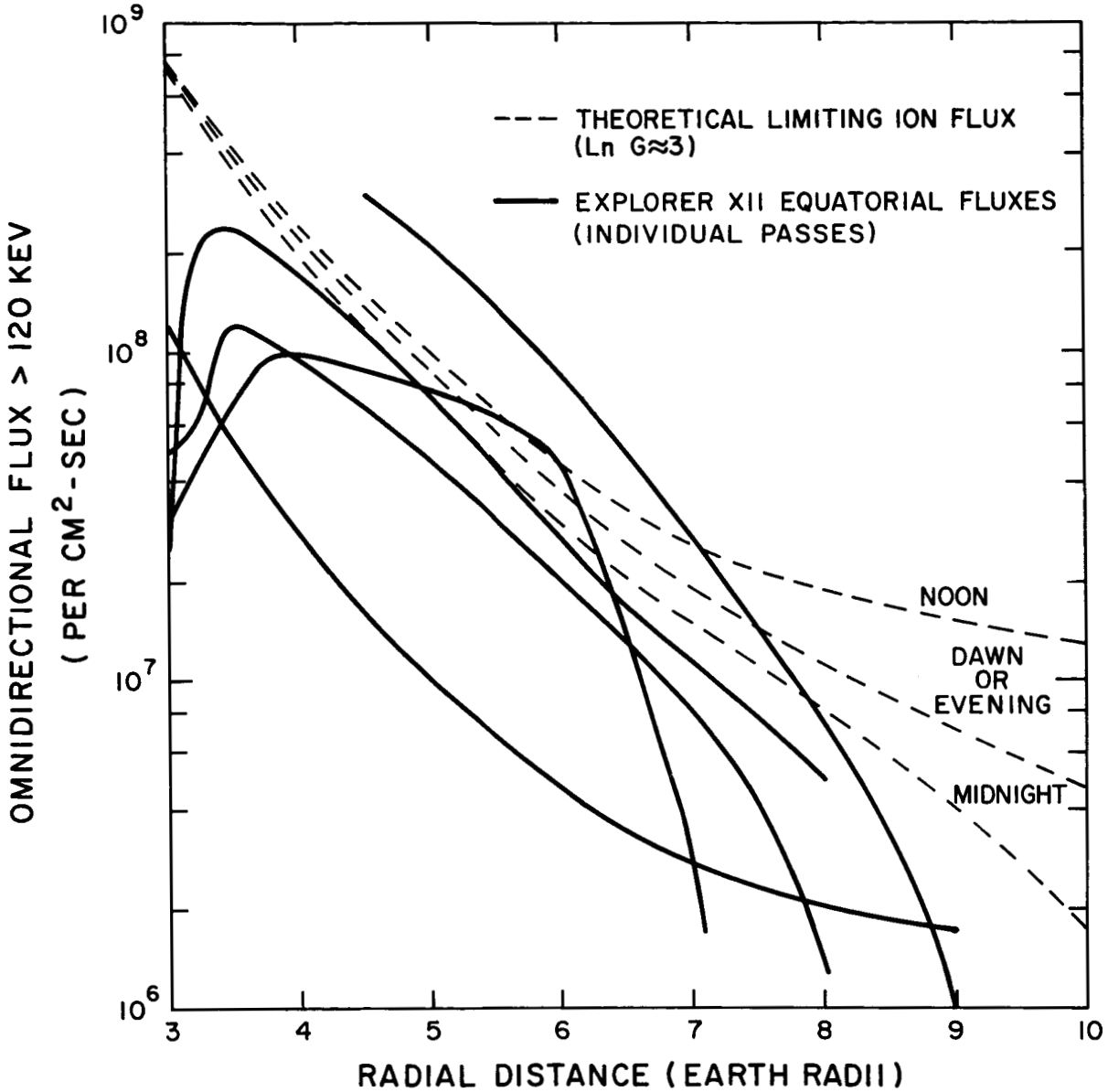

Fig. 5 Limitation on trapped protons. Here we have superposed Explorer XII radial distributions of trapped protons with energies between 120 keV and 4.5 meV and the theoretical limiting proton flux J^* (> 120 keV). For $L > 4$ it appears that protons are also accelerated to their limiting fluxes.

by (4.9) and (4.10). If the observed particles have energies well above $B^2/8\pi N$, each energy shell will have the same pitch angle distribution so that the directional flux j inside the loss cone will have the form

$$j(\alpha, >E_R) = \int_{V_R}^{\infty} \frac{S(v)}{D^*} v^3 dv \cdot \frac{1}{z_o} \frac{I_o(z)}{I_1(z_o)} = \frac{S^*}{D^*} \frac{1}{z_o} \frac{I_o(z)}{I_1(z_o)} \qquad (7.1)$$

S^* is the rate at which flux is created by the acceleration source. Then assuming that the detectors scan a sufficiently narrow solid angle, the observed flux distribution at 1000 km can be related to (7.1) by translating to the appropriate pitch angle using the adiabatic relationship $\sin^2\alpha/B = \text{const.}$ A similar statement holds for the flux pitch angle distribution outside the loss cone. Knowing j at two points inside the loss cone defines D^* since

$$\frac{j(\alpha_1)}{j(\alpha_2)} \approx \sqrt{\frac{\alpha_2}{\alpha_1}}\, e^{\frac{\alpha_1 - \alpha_2}{\sqrt{D^* T_E}}} \qquad (7.2)$$

assuming $\alpha/\sqrt{D^* T_E} \gg 1$ or "weak" diffusion. Note that the diffusion coefficient and lifetime depend primarily logarithmically on the ratio of directional fluxes.

The Injun III precipitation data [O'Brien, 1964] contains short "splashes" where the directional flux approaches pitch angle isotropy. These "splashes" seem to be superposed on a steady weak precipitation background, or "drizzle." During drizzle, the observed fluxes typically decrease by a factor 10 between detectors which are spaced 1^o apart in equatorial pitch angle. This corresponds to a drizzle diffusion coefficient of

$$\frac{1}{D^*} \approx 3 \times 10^4 \; T_E \text{ sec.} \qquad (7.3)$$

and assuming $L = 6$, a lifetime (from (4.12))

$$T_L \approx 3 \times 10^4 \text{ sec} \tag{7.4}$$

This lifetime is in rough agreement with the estimate 10^{3-5} sec made by O'Brien, [1963] on the basis of Injun I data. There he used the observed precipitation fluxes and independent information on equatorial fluxes (which permits an estimate of the total number of trapped particles on a tube of force) to generate an approximate lifetime. We use the assumption of diffusion equilibrium and the observed pitch angle profiles and find a consistent lifetime. Both these estimates yield the "instantaneous" lifetime: in other words, the lifetime a particle would have if precipitation continued at precisely the same rate. The actual residence time of any given particle could be quite different. For instance, "splashes" and other nonsteady enhanced precipitation could reduce the residence time below its steady state "drizzle" value. On the other hand, the equatorial intensity of trapped particles may not always be sufficiently great to allow precipitation to occur, thus lengthening the residence time.

Some idea of the long term behavior of the pitch angle distribution may be obtained from the median flux distributions in B and L (which is equivalent to a pitch angle distribution) both inside and outside the loss cone recently published by Armstrong, [1964]. The detector on Injun III oriented along the magnetic field saw electrons primarily in the loss cone. Since this detector had an opening angle of 43°, all the electrons detected were in the loss cone for $B > 0.27$ Gauss roughly. From these loss cone distributions, we can compute the diffusion coefficient and lifetime as before. These estimates are summarized in Table 2. Knowing the diffusion coefficient D^* and the equatorial gyrofrequency we can compute the equatorial wide band whistler mode intensity using 3.10. These are also listed in Table 2 but are not discussed until Section 8.

TABLE 2

L	4	5	6	7
Lifetime based on Median distribution	10^4 sec	3×10^4 sec	5×10^4 sec	7×10^4 sec
Required whistler intensity	2×10^{-2} γ	10^{-2} γ	8×10^{-3} γ	6×10^{-3} γ

We conclude that the median pitch angle profiles in the loss cone are also consistent with the lifetime estimates, and that therefore 40 keV electrons are often diffusion limited for $L > 4$.

Armstrong's, [1964] median 40 keV electron pitch angle distributions outside the loss cone are also consistent with a diffusion equilibrium profile. This distribution should have the form

$$j(>E_R, \alpha) = \frac{S^*}{D^*} \left\{ h(\alpha_o) + \ln \frac{\sin\alpha}{\sin\alpha_o} \right\} \tag{7.5}$$

The omnidirectional flux is

$$J(>E_R) = \frac{4\pi S^*}{D^*} \int_{\alpha_o}^{\pi/2} \left\{ h(\alpha_o) + \ln \frac{\sin\alpha}{\sin\alpha_o} \right\} \sin\alpha \, d\alpha \tag{7.6}$$

For weak diffusion, S^*/D is related to J^* as follows

$$\frac{S^*}{D^*} \approx \frac{J^*}{4\pi \ln(2/e\,\alpha_o)} \tag{7.7}$$

The arguments of Section 5 permit an estimate of J^*, and therefore S^*/D, without precise knowledge of the acceleration source. Using these values of J^* we can then predict the equatorial trapped electron pitch angle

distribution in diffusion equilibrium. The adiabatic pitch angle transformation then permits comparison with Armstrong's, [1964] data. In Figure 6 we show this computed 40 keV electron pitch angle distribution for L = 5, 6, 7. Superposed are the median >40 keV electron fluxes observed on Injun III over each range. The distribution with pitch angle of observed median fluxes near but outside the loss cone appears to have a slope consistent with the log (sin α) distribution calculated for weak diffusion equilibrium. However, the median intensity is much closer to the limiting steady state intensity than would be the case in Figure 4 for the median of the equatorial omnidirectional fluxes. The general trend is similar in that L = 5 is farther away from self-limiting instability for both equatorial omnidirectional fluxes and those near the loss cone than L = 6 and 7. Moreover, there are many individual observations near the loss cone at L = 6 and 7 which are above the median and thus violate the intensity limit. This violation may be related to the unsteady splash events. Since splashes never go beyond isotropizing the pitch angle distribution in and near the loss cone, they may correspond to an impulsive increase in the diffusion coefficient. Isotropy in and near the loss cone corresponds to the strong rather than weak diffusion case which in turn allows the limiting flux outside the loss cone to increase, since the anisotropy A decreases.

In general, we expect the flux in and near the loss cone to fluctuate more with time than the equatorial flux for two reasons. First, the effects of splashes should be most pronounced near the loss cone. Secondly, the distribution in and near the loss cone is sensitive to the amount of precipitation. Particle dumping only occurs when the equatorial flux is near self-limitation. If the fluxes are always near self-limitation, observed equatorial intensities should not fluctuate much; however, small relative changes in the equatorial flux then lead to large fractional changes in the precipitation rate. In a similar vein, O'Brien, [1964] has observed that equatorial trapped intensities increase with increasing K_p far less than do precipitated intensities.

We have also compared Injun III observations of > 230 keV electrons with the theoretical pitch angle distribution outside the loss cone. For L = 4, 5, 6 and 7 nearly all fluxes observed lie below the limiting intensity. While the distribution of median fluxes lies below the limiting intensity and the median slope does not agree as well with theory as the > 40 keV case, the

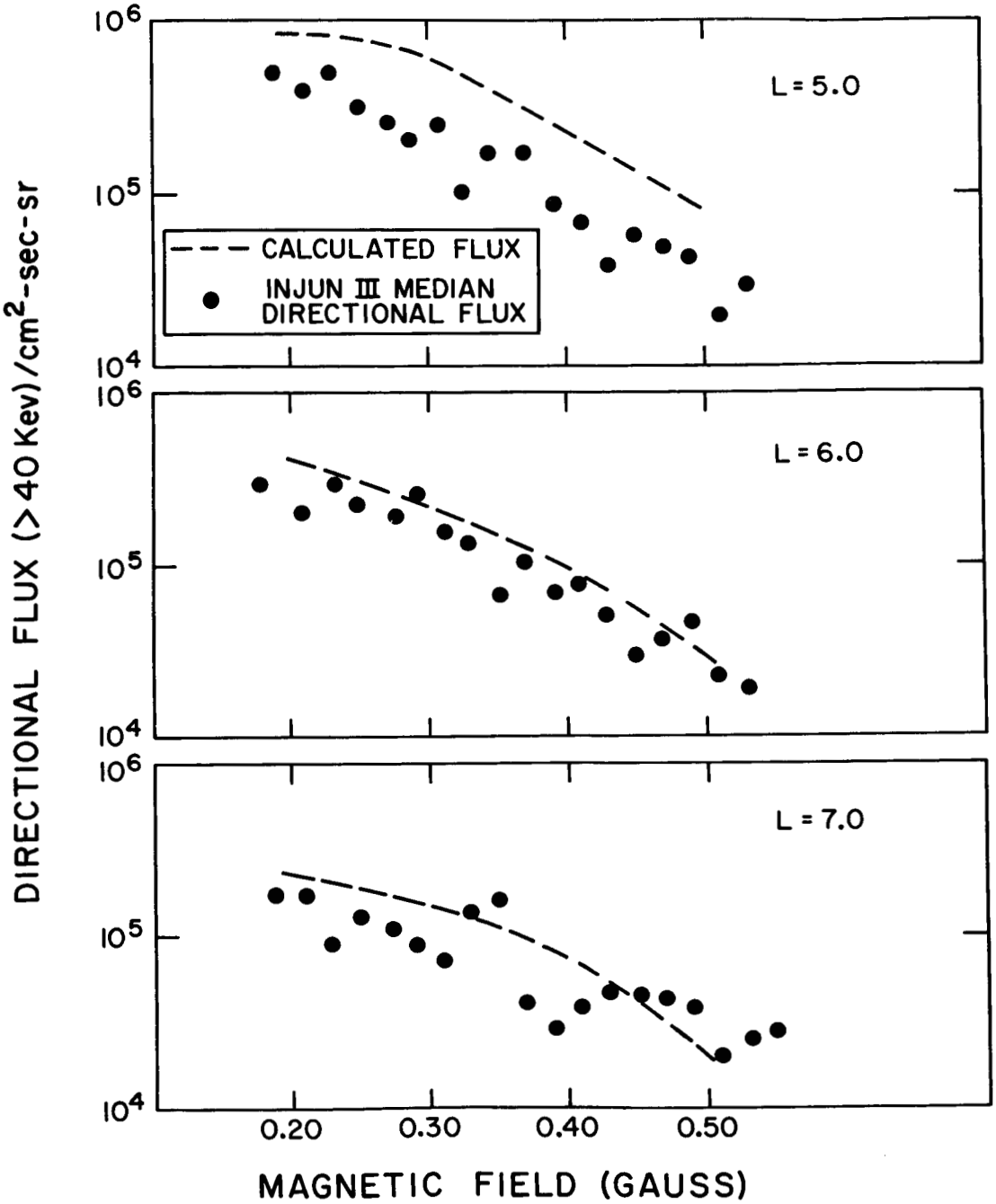

Fig. 6 > 40 keV electron pitch angle distribution outside loss cone. Shown here is a comparison in B-L coordinates of the pitch angle distribution outside the loss cone obtained with Injun III and that predicted by whistler mode diffusion theory assuming an equatorial trapped flux at its limiting intensity. The heavy points are Injun III medians for each range of $\Delta B = .02$ gauss, and the dashed line is the theoretical distribution.

distribution of maximum fluxes in an interval of B has the same rough slope and magnitude as the limiting flux. Thus, even weak diffusion probably occurs only for intense fluxes. Since the pitch angle distribution of maximum fluxes is not isotropic, we infer that splashes are probably less common for > 230 keV electrons than for > 40 keV electrons. > 1.6 meV electrons are not intense enough to approach their self-excitation limit. Their pitch angle profiles differ considerably from those at lower energies implying that these profiles are fixed by other mechanisms. This decreasing correspondence with diffusion theory as the particle energy increases is probably explainable by the statement that highly energetic particles are less often near their flux limit.

8. DISCUSSION OF EQUATORIAL VLF WAVE INTENSITY

The wide band VLF fluctuating magnetic field intensities necessary to drive the observed pitch angle diffusion are summarized in Table 2. We now can estimate the importance of wave-wave scattering mentioned in Section 3.1 as an alternate non-linear effect whose neglect would be justified in this section. Camac, et al, [1961] have estimated the rate of change of wave energy in binary wave collision as

$$\left(\frac{d\beta_w}{dt}\right)_{\text{wave-wave scattering}} \approx \omega \beta_w^2 \quad ; \quad \beta_w = (B'/B)^2 \tag{8.1}$$

Wave-wave scattering must be included when waves are sufficiently intense that the wave-scattering time becomes comparable to the wave growth time.

$$\frac{1}{\omega \beta_w} = \frac{T_w}{\ln G} \tag{8.2}$$

Using $\omega \approx 10^4$ rad/sec, and the calculated β_ω of 3×10^9, we find that $1/\omega\, \beta_w$ is 3×10^4 sec, a time long compared with $T_w/\ln G \approx 1$ sec.

At present, the only published whistler data available involves measurements taken at relatively low altitudes. Comparison with our theory therefore depends upon an extrapolation of the wave intensity predicted for the geomagnetic equator to a corresponding intensity near the Earth.

An upper limit to the wave intensity expected near the Earth assumes that all waves generated near the equator propagate completely trapped with-

out attenuation on a tube of force. Then the energy flux across a cross-sectional area A^* of the tube of force will be constant

$$\frac{(B')^2 V_G A^*}{8\pi} = \text{constant} \tag{8.3}$$

Since $\omega/|\vec{\Omega}| \ll 1$, the group velocity V_G is roughly $2\sqrt{\omega/|\vec{\Omega}|}\, V_A$. Since ω is constant, the group velocity following a wave packet is proportional to $\sqrt{B/N}$, since $A^* \sim 1/B$, then $V_G A^* \sim 1/\sqrt{BN}$. Then at an altitude of 1000 km, the wave intensity will be

$$B'(1000) \approx B'(\text{equator}) \left\{ \frac{B(1000)\, N(1000)}{B(\text{equator})\, N(\text{equator})} \right\}^{1/4} \approx L^{3/4} \left\{ \frac{N(1000)}{N(\text{equator})} \right\}^{1/4} \tag{8.4}$$

A rough estimate of the density ratio leads to $B'(1000) \approx 10B'$ (equator), and a wave intensity at 1000 km of roughly $1/10\gamma$. Gurnett and O'Brien [1964] report average chorus amplitudes between 0.5 and 7 kc/s of 8×10^{-3} γ at 1000 km and L = 5. There is therefore a factor 100 discrepancy between our predictions of wave energy based on ideal propagation and observations.

The difficulty probably lies with the ideal propagation assumption, which consists of two parts. First, the assumed perfect guiding of the tube of force increases the wave intensity by the area ratio of the flux tube (~ 200). This produces an overestimate since guidance is imperfect when the tube of force is not also a propagation duct. Secondly, although we expect wave growth at the equator, there may well be significant damping elsewhere on the propagation path. For example, the m = 0 Cerenkov resonance will always damp the wave and probably becomes important as waves move away from the equator and no longer propagate parallel to the external magnetic field.

While a direct verification of the predicted equatorial wave intensity has not been made, we can show that the predicted amplitude and the observed loss of particle energy lead to an estimate of the equatorial growth rate consistent with the requirements of diffusion theory. If the drizzle observations

correspond to a steady state, the growth rate in the equatorial region must balance the loss of waves up the line of force. Since resonant particles and waves conserve energy

$$\frac{d}{dt}\ (E_p + E_w) = 0 \tag{8.5}$$

Where E_p and E_w are the equatorial energy density in waves and resonant particles, respectively. Since $dE_w/dt = 2\gamma(B')^2/8\pi)$, we can estimate γ knowing B' and dE_p/dt. From the observed lifetime and the limiting intensity of resonant particles at the equator, we find dE_w/dt. Then we compute γ and compare it with the characteristic frequency, $1/T_w$.

Electrons random walk about a radian in their lifetime. Their parallel or perpendicular energy changes by its own order of magnitude during this time. In resonant interactions, the change in total energy is roughly $\omega/|\Omega^-|$ times the change in any component or $\Delta E \approx \omega/|\Omega^-|\ E_R$. Since there is a net diffusion flux towards the loss cone, particles deliver energy to waves, at a rate proportional to the energy loss per particle ΔE, the number of resonant particles present J/V_R, and is inversely proportional to the particle lifetime T_L.

$$\frac{dE_p}{dt} \approx - \frac{\omega}{|\Omega^-|}\ \frac{E_R J^*}{V_R T_L} \tag{8.6}$$

If $E_R \approx 40$ keV, $V_R \approx 10^{10}$ cm/sec and $\omega/|\Omega^-| \approx 0.1$. At $L = 6$, $J(>40\text{keV})$ is limited to a value $\approx 3 \times 10^7/\text{cm}^2\text{-sec}$. Choosing $T_L \approx 3 \times 10^4$ sec, the loss of particle energy density is

$$\frac{dE_p}{dt} \approx - 5 \times 10^{-16}\ \text{ergs}/\text{cm}^3\text{-sec} \tag{8.7}$$

Using the value of B' derived from the diffusion solution, $B' \approx 10^{-2}\gamma$ we infer a growth rate from the rate of change of wave energy

$$2\gamma\ \frac{(B')^2}{8\pi} \approx 5 \times 10^{-16}\ \text{ergs}/\text{cm}^3\text{-sec} \tag{8.8}$$

When $\omega/|\Omega^-| \approx 0.1$, the equatorial group velocity is roughly 2×10^9 cm/sec so that

$$\frac{1}{T_w} \approx \frac{V_G}{L R_E} \approx 0.5 \text{ rad/sec.} \tag{8.9}$$

Therefore using these rough arguments, we predict $\gamma T_w \approx 1$, whereas we used $\gamma T_w = 3$ to predict J^* in Section 5. It is clear that all these arguments are mutually consistent within their rough accuracy.

We conclude that the required wave intensities at the equator are self-consistent. No unambiguous comparison of predicted and observed wave intensities can be made at present. However, equatorial VLF measurements should be helpful in this regard.

9. SUMMARY AND DISCUSSION

For particle energies greater than $B^2/8\pi N$ the interaction of whistler noise with electrons and ion cyclotron noise with ions leads to diffusion in pitch angle. We have observed that the steady state pitch angle distribution subject to the boundary condition that particles are lost from the loss cone has an almost constant anisotropy which is of the appropriate sign to be unstable. The resultant growth rate of the waves is then directly proportional to the number of resonant particles. Since a large wave energy density leads to rapid diffusion and loss of particles, the number of trapped particles is self-limiting. Too large a particle density results in a rapid wave growth and a resultant loss of particles. As a rough criterion we have suggested that the limiting particle flux corresponds to a wave growth of a few e-foldings during traversal of the equatorial region.

While the estimate of the limiting flux is an absolute calculation without empirically adjusted constants, it does contain a number of factors each of which may be uncertain to a factor two. In particular, the anisotropy was based on a particular distribution of the source of particles, the effective length along the field line over which growth occurred was somewhat arbitrarily taken as LR_E, and finally the logarithm of the required gain may be somewhat uncertain.

The upper limit on stably trapped particle fluxes was calculated assuming a steady state "weak" diffusion model for precipitation. This model is probably adequate for a description of the long term behavior of the so-called "stably" trapped regime, i.e., those L-shells below the auroral zone on the night side, and nearly all L-shells out to the boundary of the magnetosphere on the day-side. Observations of trapped or precipitated fluxes which strongly exceed this calculated upper limit may correspond either to a non-steady state or to an exceptionally strong source. If trapped particle intensities far exeed their limit, waves could build up rapidly to create a strong diffusion regime. Because there is a minimum allowable lifetime, a sufficiently strong particle energization source can maintain strong diffusion. Then the fluxes observed may violate the weak diffusion upper limit. However, at these times, the particle pitch angle distributions will be nearly isotropic ($A \approx 0$), precipitated fluxes will then be comparable to trapped fluxes, and the particles will have their minimum lifetime T_L^*. For weaker energization sources, the weak diffusion upper limit will be obeyed.

Comparison of the weak diffusion limit with observations of electrons > 40 keV and protons > 120 keV, indicates that, with some exceptions, this upper limit is obeyed. Furthermore, in the range $L > 4$ the fluxes are close to the limit. We have not attempted to discuss a particle acceleration mechanism. The observation that the fluxes are close to the limit indicates that such a mechanism exists. However, the actual trapped flux is not determined by acceleration but by the above limit.

As a more specific illustration, the observed proton and electron fluxes are comparable implying much larger energetic proton than electron number densities. However, this does not imply a more effective acceleration mechanism for protons than for electrons. Both species are near their limiting fluxes which are the same. Therefore, the lower energetic electron number densities result from the fact that the electrons reach their number density limit earlier. It follows that the contribution of energetic ions to the ring current during magnetic storms can be as much as 40 times greater than the electron contribution.

Similarly the observations of hard energy spectra is probably related to the fact that the limiting flux is essentially independent of energy. If trapped particles are built up to their limiting flux over a range of energies the observed spectrum will be very hard. There must, of course, be some transition energy beyond which the flux is no longer near its limit and a softer spectrum exists. A rough examination of the data suggests that at L = 6 electrons at 40 keV are frequently near the limit while at 240 keV they are only occasionally at the limit.

The probable existence of a transition energy for precipitation suggests that precipitated fluxes should have a softer energy spectrum than trapped fluxes. If the spectral determination is made using observations at two energies, one above and one below the transition energy, the trapped particles will appear in both channels while precipitated particles will appear only in the lower energy channel and will thus show a softer spectrum. Of course, since precipitation occurs primarily when trapped fluxes are near their upper limit, precipitation should correlate with high overall trapped intensity. Measurements made with Injun III (Fritz, 1965) appear to support both correlations.

Several other observations support the suggestion that wave-particle interactions are indeed important. The observed distribution of particles within and near the loss cone is consistent with diffusion based on wave interactions. This suggests a typical amplitude of the magnetic field noise of 10^{-2} γ at the equator in the neighborhood of L = 6. As an internal consistency check the particle precipitation rate is sufficient to account for an energy transfer to the waves at rate consistent with the gain required in estimating the limiting flux. The above fluctuating field amplitude may be somewhat larger than observations at 1000 km altitudes might suggest. However, propagation from the equatorial interaction region to the satellite has several uncertainties. The results from satellite measurements at the equator will greatly help to clarify this point.

While resonant cyclotron interactions between whistler and ion cyclotron waves and energetic electrons and protons predict a reasonable upper limit to trapped particle intensities in rough agreement with observations, numerous phenomena have been overlooked in this gross analysis. A

number of more subtle interactions will probably need consideration in order to explain the full variety of observed phenomena. As an illustration, we mention two specific phenomena. The trapped electron flux has been observed to decrease even when its intensity is well below the self-excitation limit [Frank, Van Allen and Hills, 1964]. At first sight, this appears outside the scope of electron whistler mode interactions since wave energy cannot increase rapidly enough to overcome wave propagation losses. There are, however, at least two other possible sources of wave energy which conceivably could play a role in such a case. Wave energy could be generated on a different field line and propagate to the field line in question. Evaluation of this point requires understanding of conditions on other field lines as well as of the propagation of waves across field lines. Secondly, waves might be generated on the same field line, but at a different resonance. We have only investigated here the predominant resonance for wave growth. However, as waves move away from the equator, they will no longer propagate strictly parallel to the magnetic field, and driven velocity space diffusion at other resonances may result. Thus, wave growth due to particles at one energy could cause precipitation of particles at another energy by means of interactions occurring away from the geomagnetic equator.

We have also not discussed any effects due to structure in the frequency distribution of waves or any time dependent phenomena. For example, the limiting flux could be violated for short times since even in the strong diffusion limit, the minimum time for diffusive depopulation of the field line is the order of 10^2 sec. The strong fluctuations in precipitation fluxes as well as the fascinating variety of structured wave emissions which have been recorded indicate that more detailed time-dependent mechanisms relating specific waves and particles are required.

Acknowledgments

We are pleased to acknowledge a number of helpful discussions with W. I. Axford and N. M. Brice. This work was supported by NASA-837 and ONR-400.

REFERENCES

1. Anderson, K.A., Milton, D.W., "Balloon Observations of X-Rays in the Auroral Zone 3. High Time Resolution Studies," J. Geophys. Res., 69, 21, 4457-4480, 1964.

2. Andronov, A.A. and Trakhtengerts, V.V., "Kinetic Instability of the Earth's Outer Radiation Belt," Geomagnetism and Aeronomy, Vol. 4, No. 2, 1964. (English Translation), p. 181.

3. Armstrong, T., "The Morphology of the Outer Zone Electron Distribution at Low Altitudes from January through July and September, 1963 from Injun III," J. Geophys. Res. 70, 9, pp. 2077 - 2110, 1965.

4. Axford, W.I., Petschek, H.E. and Siscoe, G.L., "Tail of the Magnetosphere," J. Geophys. Res. 70, 5, pp. 1231-1236, 1965.

5. Brice, N., "Fundamentals of Very Low Frequency Emission Generation Mechanisms," J. Geophys. Res. 69, 21, pp. 4515-4522, 1964.

6. Brice, N.M., Private Communication.

7. Camac, M., Kantrowitz, A.R., Litvak, M.M., Patrick, R.M. and Petschek, H.E., "Shock Waves in Collision Free Plasmas," Nuclear Fusion Supplement, Part 2, pp. 423-446, 1962.

8. Carpenter, D.L. and Smith, R.L., "Whistler Measurements of Electron Density in the Magnetosphere," Reviews of Geophysics 3, pp. 415-441, 1964.

9. Chandrasekhar, S., "Plasma Physics," U. Chicago Press, Chicago, 1960.

10. Chang, D.B., "Amplified Whistlers as the Source of Jupiter's Sporadic Decameter Radiation," Ap. J., 138, 4, 1231-1241, 1963.

11. Chang, D.B. and Pearlstein, L.D., "On the Effect of Resonant Magnetic Moment Violation on Trapped Particles," General Atomics/General Dynamics Report GA-5891, 1964. Submitted to J. Geophys. Res.

12. Cornwall, J.M., "Cyclotron Instabilities and Electromagnetic Emission in the Ultralow Frequency and Very Low Frequency Ranges," J. Geophys. Res. 70, 1, pp. 61-70, 1965.

13. Davis, L.R., Hoffman, R.A., and Williamson, J.M., "Observations of Protons Trapped Above 2 Earth Radii," Trans. AGU 45, 1, p. 84, 1964, paper p. 53.

14. Davis, L.R. and Williamson, J.M., "Low Energy Trapped Protons" Space Research, III., ed. W. Priester, pp. 365-375, 1963.

15. Dragt, A.J., "Effect of Hydromagnetic Waves on the Lifetimes of Van Allen Radiation Protons," J. Geophys. Res. 66, pp. 1641-1649, 1961.

16. Drummond, W.E. and Pines, P., "Non-Linear Stability of Plasma Oscillations," Nuclear Fusion Supplement, Part 3, pp. 1049-1058, 1962.

17. Dungey, J.W., "Loss of Van Allen Electrons Due to Whistlers," Planet. Space Sci. 11, pp. 591-595, 1963.

18. Fishman, F.J., Kantrowitz, A.R. and Petschek, H.E., "Magneto-hydrodynamic Shock Wave in a Collision Free Plasma," Rev. Mod. Phys. 32, pp. 959-966, 1960.

19. Frank, L.A., Van Allen, J.A. and Macagno, E., "Charged Particle Observations in the Earth's Outer Magnetosphere," J. Geophys. Res. 68, pp. 3543-3554, 1963.

20. Frank, L.A., Van Allen, J.A., Hills, H.K., "An Experimental Study of Charged Particles in the Outer Radiation Zone," J. Geophys. Res. 69, pp. 2171-2191, 1964.

21. Frank, L.A., "A Survey of Electrons $E > 40$ keV beyond 5 Earth Radii with Explorer 14," J. Geophys. Res. 70, 7, pp. 1593-1626, 1965.

22. Freeman, J.W., "The Morphology of the Electron Distribution in the Outer Radiation Zone and Near the Magnetospheric Boundary as Observed by Explorer 12," J. Geophys. Res. 69, pp. 1691-1723, 1964.

23. Fritz, T.A., "A Statistical Study of the Electron Energy Spectrum between 40 and 100 keV in the Outer Zone," paper P140, 46th Annual Meeting, AGU, April 19-22, 1965. Trans. AGU 46, 1, p. 138, 1965.

24. Gurnett, D.A. and O'Brien, B.J., "High Latitude Studies with Satellite Injun III, 5. Very-Low-Frequency Electromagnetic Radiation," J. Geophys. Res. 69, 1, pp. 65-90, 1964.

25. Hartz, T.R., Montbriand, L.E. and Vogan, E.L., "A Study of Auroral Absorption at 30 mc/s," Can. J. Phys. 41, pp. 581-595, 1963.

26. Jacobs, J.A. and Watanabe, T., "Micropulsation Whistlers," J. Atmospheric Terrest. Phys. 26, pp. 825-829, 1964.

27. Kadomtsev, B.B. and Petviashvili, V.I., "Weakly Turbulent Plasma in a Magnetic Field," Sov. Phys. JETP, 16, 6, pp. 1578-1585, 1963.

28. McDiarmid, I. B., Burrows, J. R., Budzinski, E. E. and Wilson, M. D., "Some Average Properties of the Outer Radiation Zone at 1000 km," Can. J. Phys. 41, pp. 2064-2079, 1963.

29. McDiarmid, I. B., and Budzinski, E. E., "Angular Distributions and Energy Spectra of Electrons Associated with Auroral Events," Can. J. Phys. 42, 11, pp. 2048-2062, 1964.

30. Obayashi, T., "Hydromagnetic Whistlers," J. Geophys. Res. 70, 5, pp. 1069-1079, 1965.

31. O'Brien, B. J., "Lifetimes of Outer Zone Electrons and their Precipitation into the Magnetosphere," J. Geophys. Res. 67, pp. 3687-3706, 1962.

32. O'Brien, B. J., "High Latitude Geophysical Studies with Satellite Injun III 3. Precipitation of Electrons into the Atmosphere," J. Geophys. Res. 69, 1, pp. 13-44, 1964.

33. Sagdeev, R. Z. and Shafronov, V. D., "On the Instability of a Plasma with an Anisotropic Distribution of Velocities in a Magnetic Field," Soviet Physics, JETP 12, 1, pp. 130-132, 1961.

34. Stix, T. H., The Theory of Plasma Waves, McGraw-Hill, New York, 1962.

35. Sturrock, P. A., "Nonlinear Effects in Electron Plasmas," Proc. Roy. Soc., A., 242, pp. 277-299, 1957.

36. Vedenov, A. A., Velikhov, E. P. and Sagdeev, R. Z., "Quasi-Linear Theory of Plasma Oscillations," Salzburg, 1961, Nuclear Fusion Suppl. 2, pp. 465-475, 1962.

37. Wentzel, D. G., "Hydromagnetic Waves and Trapped Radiation, part 1, Breakdown on the Adiabatic Invariance," J. Geophys. Res. 66, pp. 359-362, 1961. "Displacement of the Mirror Points," J. Geophys. Res. pp. 363-369, 1961.

38. Winckler, J. R., Bhavsar, P. D. and Anderson, K. A., "A Study of the Precipitation of Energetic Electrons from the Geomagnetic Field During Magnetic Storms," J. Geophys. Res. 67, pp. 3717-3736, 1962.